A MONTE CARLO METHOD FOR THE CALCULATION OF THE SURFACE TENSION OF AIR-WATER AND LIPID-WATER INTERFACES

By

CHYUAN-YIH LEE

Bachelor of Science
National Chiao-Tung University
Hsinchu, Taiwan
1970

Master of Science
Tamkeng College of Arts and Sciences
Tamsui, Taiwan
1974

Submitted to the Faculty of the Graduate College
of the Oklahoma State University
in partial fulfillment of the requirements
for the Degree of
DOCTOR OF PHILOSOPHY
December, 1980

A MONTE CARLO METHOD FOR THE CALCULATION OF THE SURFACE TENSION OF AIR-WATER AND LIPID-WATER INTERFACES

Thesis Approved:

Hugh L. Scott
Thesis Adviser

Paul Worthington

L. J. Dunn

J P Chandler

Norman N Durham
Dean of the Graduate College

ACKNOWLEDGMENTS

The author wishes to express his appreciation to his major adviser, Dr. H. L. Scott, for the suggestion of this problem and for his professional guidance, assistance, and time for discussion throughout the course of this study. Thanks are extended to Dr. J. P. Chandler for his improving the computer program used in this study, and to other committee members, Dr. P. A. Westhaus and Dr. H. J. Harmon, for their help and advice. Mrs. Janet Sallee is also appreciated for the excellence of the final copy.

The author gratefully acknowledges the financial support provided by the National Science Foundation and the computer facility of the Oklahoma State University.

Special gratitude is expressed to my mother for her encouragement, sacrifice and understanding through the years and to my wife, Chiou-Song, for her love and inspiration.

TABLE OF CONTENTS

Chapter		Page
I.	INTRODUCTION.	1
	Basic Concept of Surface Tension	1
	Water-Water Pair Potentials.	6
	ST2 Potential	6
	CI Potential.	8
	The Metropolis Monte Carlo Method.	10
	Purpose of This Study.	12
II.	UMBRELLA SAMPLING	13
	Torrie-Valleau's Umbrella Sampling	13
	Half-Umbrella Sampling	17
III.	PROCEDURE FOR THE CALCULATION OF THE SURFACE TENSION. . .	20
	Outline of the Procedure	20
	The Main Contribution: $F_c - F_b$	21
	Contribution From Long-Range Interactions.	24
	Contribution From Relaxing the Hard Wall Constraint.	26
IV.	COMPUTATIONAL DETAILS	28
	Initial Configuration.	28
	Calculation of Potential Energy.	30
	Trial Move of a Molecule	33
	Acceptance or Rejection of the Trial Move.	33
	Location of the Important Regions.	34
V.	MODEL SYSTEMS STUDIED AND THEIR RESULTS	36
	Air-Water Interfaces	36
	The Main Contribution $F_c - F_b$	36
	The Long Range Contribution	37
	The Relaxation Contribution $F_d - F_c$	39
	Lipid-Water Interfaces	39
VI.	DISCUSSION AND CONCLUSION	48
REFERENCES.	. . . . .	52
APPENDIX A.	DERIVATION OF KIRKWOOD-BUFF FORMULA.	54

Chapter Page

APPENDIX B. THE METROPOLIS MONTE CARLO WALK AS A MARKOV CHAIN. . 58

APPENDIX C. COMPUTER PROGRAM FOR THE CALCULATION OF THE FREE ENERGY CHANGE IN SEPARATING SLAB SHAPED LIQUIDS. . . 62

APPENDIX D. ORIENTATION OF THE WATER MOLECULES NEAR SURFACE. . . 73

LIST OF TABLES

Table		Page
I.	Free Energy Differences and Important Ranges in Energy as a Function of the Separation Distance Between Slabs. . .	38
II.	Systems Studied and Resulting Surface Tension Values . . .	45

LIST OF FIGURES

Figure — Page

1. Illustration of the Surface Tension From a Molecular Point of View 2

2. Diagrams for the ST2 and CI Potentials. (a) The ST2 Model Where the Water Molecule is Represented by Four Point Charges, θ_t Being the Tetrahedral Angle. (b) Definition of Indices Used in the CI Potential. The M Point Lies on the Molecular C_2 Azis. $R_{OM} = 0.2677\mathring{A}$, $R_{OH} = 0.9572\mathring{A}$, $\angle HOH = 104.5^{o}$ 7

3. Properties of Configuration Space for the System of 32 Lennard-Jones Particles. (a) Solid Line: $f(\Delta U^*)$; Dashed Line: $f(\Delta U^*)\exp(-\Delta U^*)$. (b) Solid Line: the Desired $f_W(\Delta U^*)$ in the Torrie-Valleau Sampling; Broken Line (- · - · - ·): W Obtained From Eq. (25), $f_W(\Delta U^*)$ and $f(\Delta U^*)$ in (a); Left Dashed Line: $[\exp(-\Delta U^*)/W]f_W(\Delta U^*)$; Right Dashed Line: $f_W(\Delta U^*)/W$. (c) Solid Line: $f_{1/2}(\Delta U^*)$; Left Dashed Line: $f_{1/2}(\Delta U^*)\exp(-\Delta U^*/2)$; Right Dashed Line: $f_{1/2}(\Delta U^*)\exp(\Delta U^*/2)$. Left Scales are for Solid and Broken Lines, Right Scales are for Dashed Lines. The Horizontal Scale is the Same for All Figures. 15

4. Behavior of Monte Carlo Samplings. Dashed Line Represents the Metropolis Monte Carlo Sampling and Solid Line Represents the Half-Umbrella Sampling. Both Start From a Configuration With ΔU^* Ground the Most Probable Position, ΔU^*_{mo}, of the Metropolis Monte Carlo Walk. 19

5. The Modified Periodic Boundary Conditions 23

6. Flow Chart of the Half-Umbrella Sampling. 29

7. Definition of the Body Frame for the ST2 Water Molecule . . 31

8. Schematic Representation of the Lipids Spreading at Air/Water Interface. The Zig-Zag Lines Represent the Hydrocarbon Chains and the Circles Represent Head Groups . . . 41

9. The Head Group of Phosphatidylcholine 42

10. Top and Side Schematic Views of the Systems Simulated. The Arrows Represent Head Group Dipoles and the Circles Represent Water 44

Figure Page

11. A Plot of the Ratio of the Calculated Film Surface Tension to the Calculated Water Surface Tension Vs. Effective Dipole Moment of the Head Group. Error Bars are ± 0.06 (± 6 Dynes/cm) 47

12. Orientational Distribution of the Surface Water Using ST2 Potential. The θ Angle is Divided Into 32 Regions and the Vertical Axis Represents the Percentage of the Monte Carlo Steps Falling Into Each Region 75

13. Orientational Distribution of the Surface Water Using CI Potential. The θ Angle is Divided Into 32 Regions and the Vertical Axis Represents the Percentage of the Monte Carlo Steps Falling Into Each Region 76

CHAPTER I

INTRODUCTION

Basic Concept of Surface Tension

Aqueous interfaces are of considerable importance in many biological and chemical systems (1,2). In particular, cell surfaces consist of a water/membrane interface for which very little quantitative detail is available. A key quantity in the characterization of interfaces is the surface tension.

Surface tension can be viewed as the force tending to contract a surface area. The origin of this contracting force is illustrated in Figure 1. We note that a molecule in the interior of a liquid is attracted isotropically by its neighbors. However, a molecule very near or actually in the interface between the liquid and a gas experiences a net attractive force directed inward and normal to the surface. Suppose initially the concentration of the molecules at the surface is the same as that in the interior, then molecules will be pulled into the interior until the concentration gradient at the surface sets up a chemical force which is sufficient to cancel this tendency. Since a smaller concentration means a smaller pressure, the pressure P' at the interface should be smaller than the pressure P at other regions. Let ΔF_x be the x-component of the force due to the pressure difference and b be the length, in the y direction, of the container shown in Figure 1 (ab being the surface area). Then the surface tension is defined by

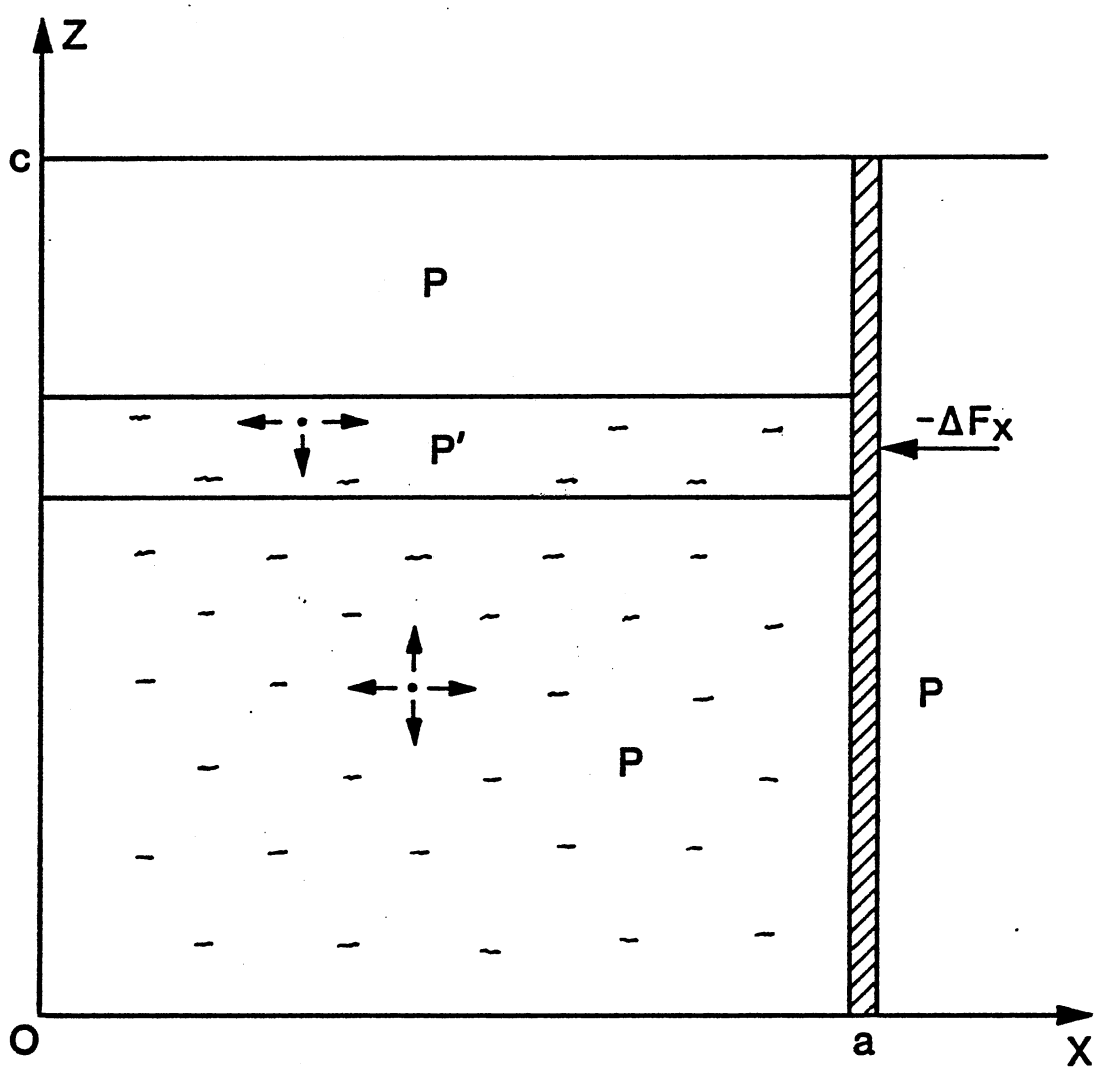

Figure 1. Illustration of the Surface Tension From a Molecular Point of View

$$\gamma \equiv -\Delta F_x/b \tag{1}$$

(3,4). From the mechanical definition, one can obtain (see Appendix A) the Kirkwood-Buff formula (3,5),

$$\gamma = \frac{1}{A} < \sum_{i>j} \frac{(x_{ij}^2 - z_{ij}^2)}{r_{ij}} u'(r_{ij}) > \tag{2}$$

where A represents the surface area, r_{ij} is the distance between ith and jth molecules, <> denotes the canonical ensemble average, $u'(r_{ij})$ is the derivative of the pair potential $u(r_{ij})$, and $x_{ij} = x_i - x_j$, $z_{ij} = z_i - z_j$.

Alternatively, the surface tension can be viewed as the excess Helmholtz free energy over the bulk system. We have seen that the surface tension tends to contract a surface area. Thus, in order to create a new surface area ΔA by an isothermal and reversible process, it is necessary to do an amount of mechanical work, $\gamma\Delta A$, against the surface tension. As the surface area is created, the molecules at the surface will become farther apart. This moving-apart of the molecules is aided by their thermal motions. During this process, the molecules lose kinetic energy so that, in order to keep the temperature constant, it is necessary to supply an equivalent amount of heat from the surroundings. In a reversible process, the heat is equal to $T\Delta S$, where ΔS is the entropy change accompanying the creation of the surface area and T is the absolute temperature. Therefore, according to the first law of thermodynamics, the total energy required for the creation of surface area is given by

$$\Delta E = \gamma\Delta A + T\Delta S$$

or

$$\gamma = (\Delta E - T\Delta S)/\Delta A = \Delta F/\Delta A \tag{3}$$

where ΔF is the change of Helmholtz free energy associated with the creation of surface area.

In statistical mechanics (6), the Helmholtz free energy is given by

$$F \equiv - kT \ln Q \equiv - kT \ln \int e^{-U(q^N)/kT} \, dq^N \tag{4}$$

where k is Boltzmann constant, U is the potential energy and Q denotes the partition function (configuration integral). Then, the free energy difference between any two systems "0" and "1" can be written

$$\Delta F \equiv F_1 - F_0 = - kT \ln \frac{\int e^{-U_1/kT} \, dq^N}{\int e^{-U_0/kT} \, dq^N}$$

$$= - kT \ln \frac{\int e^{-(U_1-U_0)/kT} \cdot e^{-U_0/kT} \, dq^N}{\int e^{-U_0/kT} \, dq^N}$$

$$\equiv - kT \ln \langle e^{-\Delta U^*} \rangle_0 \tag{5}$$

where $\langle\rangle_0$ is the canonical ensemble average over all configurations of the system 0, and

$$\Delta U^* \equiv (U_1 - U_0)/kT \tag{6}$$

The free energy difference can also be obtained by the Bennett formula (7),

$$F_1 - F_0 = - kT \ln \frac{\langle M(\Delta U^*) \rangle_0}{\langle M(-\Delta U^*) \rangle_1} \tag{7}$$

where $M(x) \equiv \min\{1, \exp(-x)\}$. Equation (7) is derived from the following identity,

$$M(x)/M(-x) = e^{-x}$$

or more specifically,

$$M(\Delta U^*)\ e^{-U_0/kT} = M(-\Delta U^*)\ e^{-U_1/kT} \tag{8}$$

Integrating this identity over all configuration space and multiplying by the trivial factors, Q_0/Q_0 and Q_1/Q_1 (Q_0 and Q_1 are the configuration integrals of systems 0 and 1, respectively), one obtains

$$Q_0 \frac{\int M(\Delta U^*)\ e^{-U_0/kT}\ dq^N}{Q_0} = Q_1 \frac{\int M(-\Delta U^*)\ e^{-U_1/kT}\ dq^N}{Q_1} \tag{9}$$

Equation (9) can be written as

$$Q_1/Q_0 = \langle M(\Delta U^*) \rangle_0 / \langle M(-\Delta U^*) \rangle_1 \tag{10}$$

which leads to Equation (7).

In the last decade, two fairly realistic intermolecular potentials have been developed for water (8,9). The detailed analytical forms are given in the following section.

Water-Water Pair Potentials

ST2 Potential

The ST2 water molecule (8) contains four point charges. Its geometry is shown in Figure 2a. The positive charges +q are identified as protons, located 1Å from the oxygen nucleus 0. The distance from 0 to each of the negative charges -q is 0.8Å. The angels between any two vectors connecting 0 to the point charges are all equal to the tetrahedral angel θ_t,

$$\theta_t = 2 \cos^{-1} (3^{-1/2}) = 109^{\circ}28' \tag{11}$$

The interaction potential between two ST2 molecules is given by

$$u_{ST2} = V_{LJ}(r_{ij}) + G(r_{ij})\, V_{el}(i,j) \tag{12}$$

where r_{ij} denotes the oxygen-oxygen distance and

$$\begin{aligned} V_{LJ}(r_{ij}) &= 4\varepsilon[(\sigma/r_{ij})^{12} - (\sigma/r_{ij})^{6}] \\ V_{el}(i,j) &= q^2 \sum_{m,n=1}^{4} (-1)^{m+n}/d_{mn}(i,j) \end{aligned} \tag{13}$$

with $d_{mn}(i,j)$ the distance between charge m on molecule i and charge n on molecule j (m and n are even for positive charges, odd for negative charges). The modulation function G is given by

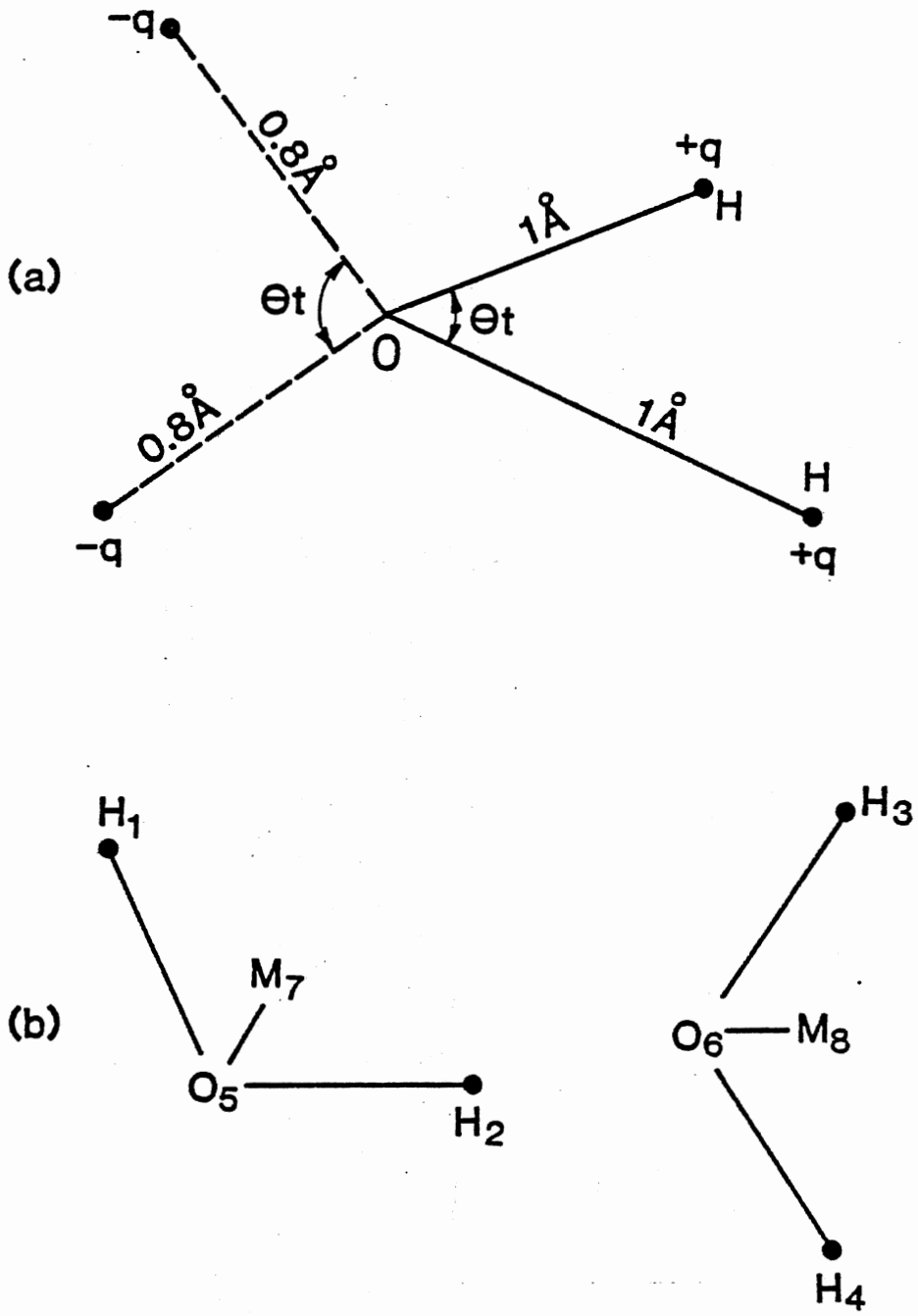

Figure 2. Diagrams for the ST2 and CI Potentials. (a) The ST2 Model Where the Water Molecule is Represented by Four Point Charges, θ_t Being the Tetrahedral Angle. (b) Definition of Indices Used in the CI Potential. The M Point Lies on the Molecular C_2 Axis. R_{OM} = 0.2677Å, R_{OH} = 0.9572Å, <HOH = 104.5°

$$G(r_{ij}) = 0 \qquad 0 \le r_{ij} \le R_L$$

$$= \frac{(r_{ij} - R_L)^2 (3R_U - R_L - 2r_{ij})}{(R_U - R_L)^2} \qquad R_L \le r_{ij} \le R_U$$

$$= 1 \qquad R_U \le r_{ij} \qquad (14)$$

The parameters have the following values:

$$\varepsilon = 5.2605 \times 10^{-15} \text{ erg}; \qquad \sigma = 3.10 \text{ Å}$$

$$q = 0.2357 \ e = 1.13194 \times 10^{-10} \text{ esu}$$

$$R_L = 2.0160 \text{ Å}, \qquad R_U = 3.1287 \text{ Å}$$

The ST2 potential was obtained by semiempirical means (8). Its radial distribution function is in good agreement with experiments (8, 10, 11). The potential energy of ST2 water is about - 10.5 kcal/mole at 25°C (11). When the kinetic energy of 1.8 kcal/mole (= 3 RT) is added, the internal energy of ST2 water becomes - 8.7 kcal/mole, which is slightly lower than the experimental value, - 8.1 kcal/mole (12). The heat capacity was calculated to be 26 cal/mole/deg (11), compared with the experimental value of 18 cal/mole/deg (= 1 cal/gm/deg).

CI Potential

The CI (configuration interaction) potential (9) takes the following form,

$$u_{CI} = q^2(1/R_{13} + 1/R_{14} + 1/R_{23} + 1/R_{24} + 4/R_{78} - 2/R_{18} - 2/R_{28}$$

$$- 2/R_{37} - 2/R_{47}) + a_1 \exp(-b_1 R_{56}) + a_2[\exp(-b_2 R_{13})$$

$$+ \exp(-b_2 R_{14}) + \exp(-b_2 R_{23}) + \exp(-b_2 R_{24})]$$

$$+ a_3[\exp(-b_3 R_{16}) + \exp(-b_3 R_{26}) + \exp(-b_3 R_{35})$$

$$+ \exp(-b_3 R_{45})] - a_4[\exp(-b_4 R_{16}) + \exp(-b_4 R_{26})$$

$$+ \exp(-b_4 R_{35}) + \exp(-b_4 R_{45})] \qquad (15)$$

where R_{ij} denotes the distance between a pair of atoms shown in Figure 2b, and

$a_1 = 1.088931 \times 10^6$ kcal/mole; $a_2 = 6.667210 \times 10^2$ kcal/mole

$a_3 = 1.455685 \times 10^3$ kcal/mole; $a_4 = 2.736156 \times 10^2$ kcal/mole

$b_1 = 5.152759$ Å^{-1}; $b_2 = 2.760870$ Å^{-1}

$b_3 = 2.961927$ Å^{-1}; $b_4 = 2.233281$ Å^{-1}

$q^2 = 170.8842$ kcal-Å/mole

These parameters were chosen to give a best fit to the energies obtained by ab initio configuration interaction calculations on a set of 66 water dimer configurations (9). The CI potential is then a true interaction potential (not the effective one) between two water molecules. Since quantum mechanical many-body interactions are not taken into account, it is not surprising that the calculated internal energy, - 6.8 kcal/mole (11,13), is higher than the experimental value, - 8.1 kcal/mole. The resulting radial distribution functions, however, are in excellent agreement with experiments (11,13). The heat capacity was calculated to be 20 cal/mole/deg (11).

Because both intermolecular potentials are so complex, it is impractical to carry out, by the usual numerical methods, the integrals involved in the surface tension calculation. For this reason it is natural to consider computer simulations. In the last decade, the Monte Carlo method has been used to calculate the surface tension of argon, which was assumed to obey the Lennard-Jones potential,

$$V_{LJ}(r) = 4\varepsilon\left[(\sigma/r)^{12} - (\sigma/r)^{6}\right] \tag{16}$$

where σ and ε are constants (14-16). The surface tension of water, however, has not been calculated by the Monte Carlo method so far as we know. In the next section, we describe a Monte Carlo method developed by Metropolis et al. (17).

The Metropolis Monte Carlo Method

Since 1953, canonical ensemble averages have been frequently evaluated by the Metropolis Monte Carlo method (17). The general procedure is:

(i) Place the particles of the system in any configuration.

(ii) Move one of the particles according to $q_j \rightarrow q_j + \xi_j \delta q_j$, where q_j is the j-th coordinate for the particle, δq_j is the maximum allowed displacement and ξ_j is a random number between -1 and 1.

(iii) Calculate the potential energy change, $\delta U (\equiv U_{new} - U_{old})$, caused by the move.

(iv) If $\delta U \leq 0$, the transition is accepted and the particle is placed in its new position. If $\delta U > 0$, we compare $\exp(-\delta U/kT)$ with a random number η between 0 and 1. If

$\exp(-\delta U/kT) > \eta$, the transition is accepted; if $\exp(-\delta U/kT) \leq \eta$, the transition is rejected and the particle is returned to its old position.

(v) Iterating the above procedure for a sufficiently large number of steps. If g_t is the value of the function g at t-th step, then it can be shown (see Appendix B) that

$$\langle g \rangle = \lim_{n\to\infty} \frac{1}{n} \sum_{t=1}^{n} g_t \qquad (17)$$

In practice, n is finite but large enough to make the fluctuation of the Monte Carlo average as small as we desire. From procedure (iv) we see that, regardless of the initial configuration, the system will eventually reach "equilibrium", that is, the Monte Carlo walk concentrates on the configurations with lower potential energies. The speed with which the system approaches equilibrium depends on the maximum allowed displacement δq_j. If δq_j is too large, most trial moves will be rejected, and if too small the configuration will not change enough. Usually δq_j is chosen so that about half of the trial moves are accepted. The speed of convergence of the Monte Carlo average also depends on the function to be measured. If the function (such as potential energy, radial distribution function or order parameter) changes slowly at equilibrium, good accuracy (within 3%) can be obtained for $n = 10^5 - 10^6$ (10,18). However, for the calculation of surface tension, we note that Equation (2) contains <u>derivative</u> of $u(r_{ij})$ which may vary sharply with r_{ij}. The presence or absence of certain configuration for which u' is large would strongly influence the Monte Carlo average. For particles obeying Lennard-Jones potential the surface tension calculated by

Equation (2) has been found to fluctuate over a wide range (~ 14%) even for $n = 6 \times 10^6$ (14). In our preliminary studies, we have attempted to use Equation (2) to calculate the surface tension of water but failed to obtain a stable value using either the ST2 or CI potential.

Purpose of This Study

The goal of this work is to develop an efficient method to calculate the surface tension using the free energy definition. We note that both Equations (5) and (7) contain exponential functions which also vary rapidly with configurations. The convergence of the Monte Carlo average is expected to be poor. To improve this convergence, Torrie and Valleau (19,20) suggested a sampling technique called "umbrella sampling", in which a weighting function, determined by trial and error, is introduced to sample the g_t's so that the Monte Carlo average converges faster. In Chapter II we describe this method in more detail. In our conputation we shall use a similar but more straightforward technique also described in Chapter II. The technique is then applied to the study of the surface tension of air-water and lipid-water interfaces. The detailed procedure and computations are given in Chapter III and Chapter IV. Chapter V gives the results of our calculations and Chapter VI contains the conclusions and discussions. In Appendix D we also include the results on the orientation of water molecules near surface.

CHAPTER II

UMBRELLA SAMPLING

Torrie-Valleau's Umbrella Sampling

In the previous chapter, we derived three different formulas, Equations (2), (5) and (7) for the Monte Carlo calculation of surface tension. However, we also pointed out that the traditional Monte Carlo method is not efficient in all of the three cases. Over the past few years, an alternative algorithm has been proposed to calculate the term, $\langle e^{-\Delta U^*} \rangle_0$, involved in Equation (5), where ΔU^* is the potential energy difference in unit kT between any two systems, 0 and 1. This algorithm is based on the following idea.

Let $m(\Delta U^*)$ be the number of the Metropolis Monte Carlo steps with ΔU^* falling between ΔU^* and $\Delta U^* + d\Delta U^*$. Then for the calculation of $\langle e^{-\Delta U^*} \rangle_0$, Equation (17) becomes

$$\langle e^{-\Delta U^*} \rangle_0 = \lim_{n\to\infty} \frac{1}{n} \int_{-\infty}^{\infty} e^{-\Delta U^*} m(\Delta U^*) d\Delta U^*$$

$$= \int_{-\infty}^{\infty} f(\Delta U^*)\ e^{-\Delta U^*}\ d\Delta U^* \qquad (18)$$

where

$$f(\Delta U^*) \equiv \lim_{n\to\infty} \frac{m(\Delta U^*)}{n} \qquad (19)$$

is the probability density function of ΔU^*. For the best efficiency of

sampling, the Monte Carlo walk should concentrate on the region where the integrand, $F(\Delta U^*) = f(\Delta U^*)\exp(-\Delta U^*)$, is large. Unfortunately, as pointed out by Torrie and Valleau (20) the maximum of $f(\Delta U^*)$ is unlikely to be the maximum of $F(\Delta U^*)$. The two functions are depicted in Figure 3a for the free energy difference between the following two systems.

$$U_1 = 4\varepsilon \sum_{i<j}^{N} [(\sigma/r_{ij})^{12} - (\sigma/r_{ij})^{6}] \tag{20}$$

$$U_0 = 4\varepsilon \sum_{i<j}^{N} (\sigma/r_{ij})^{12} \tag{21}$$

where N is the number of particles in a unit cell (simple cubic periodic boundary conditions are used), and ε and σ are constants. In this example, N = 32, ε = 0.365 kT, and the length of cubic unit cell = 3.35 σ. We note that $f(\Delta U^*)$ is of umbrella shape and its slope becomes steeper and steeper on both sides of the most probable position, ΔU^*_{mo}. Thus, $f(\Delta U^*)$ is small at the region where $F(\Delta U^*)$ is large. This makes it very difficult to sample this region. To improve the sampling efficiency, let us consider the following identity:

$$\langle g \rangle_0 \equiv \frac{\int g\, e^{-U_0/kT}\, dq^N}{\int e^{-U_0/kT}\, dq^N}$$

$$= \frac{\int (g/W) W\, e^{-U_0/kT}\, dq^N}{\int (1/W) W\, e^{-U_0/kT}\, dq^N}$$

$$= \frac{\int (g/W) W\, e^{-U_0/kT}\, dq^N}{\int W\, e^{-U_0/kT}\, dq^N} \times \frac{\int W\, e^{-U_0/kT}\, dq^N}{\int (1/W) W\, e^{-U_0/kT}\, dq^N}$$

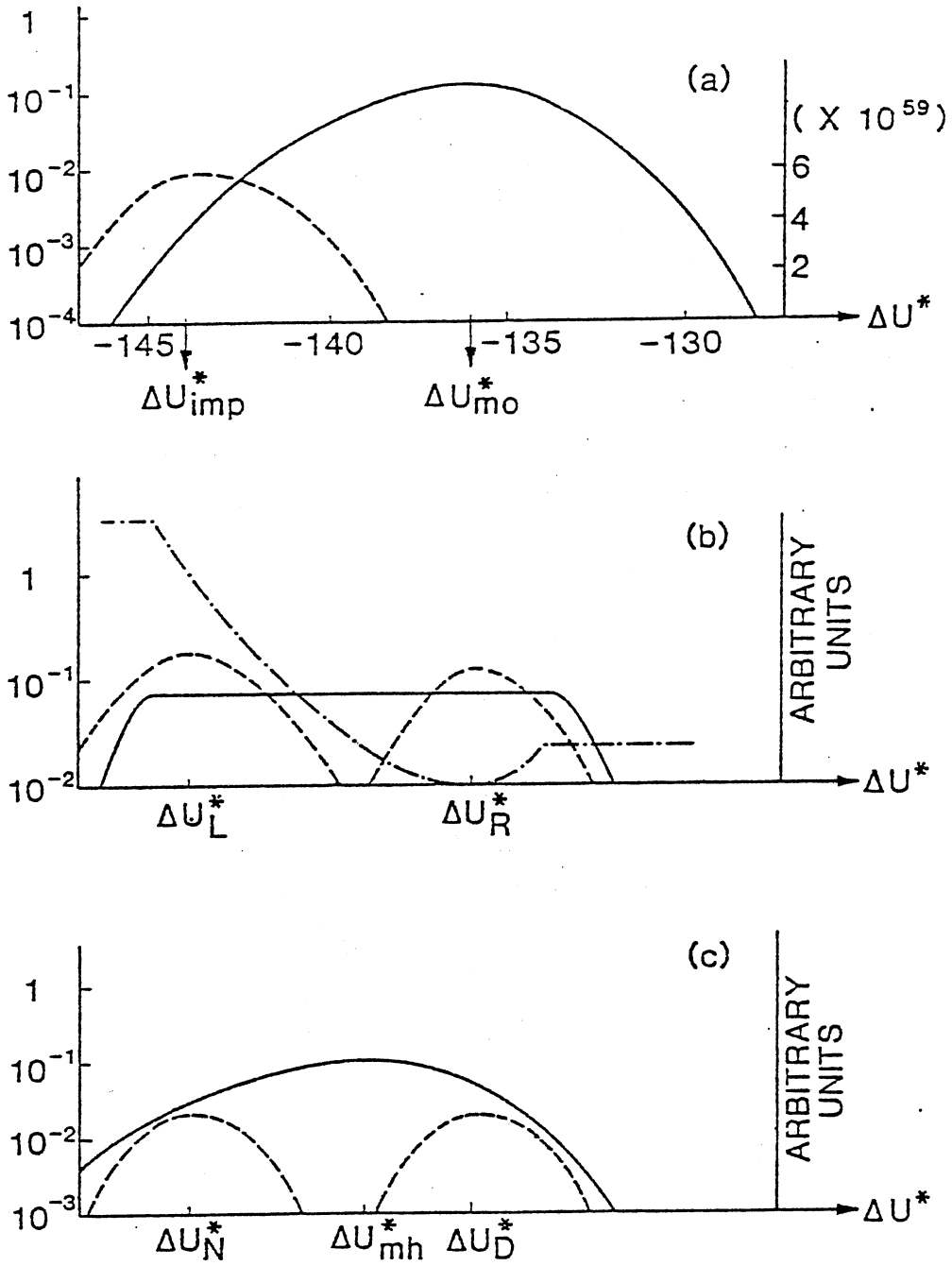

Figure 3. Properties of Configuration Space for the System of 32 Lennard-Jones Particles. (a) Solid Line: $f(\Delta U^*)$; Dashed Line: $f(\Delta U^*)\exp(-\Delta U^*)$. (b) Solid Line: the Desired $f_W(\Delta U^*)$ in the Torrie-Valleau Sampling; Broken Line (- · - · - ·): W Obrained From Eq. (25), $f_W(\Delta U^*)$ and $f(\Delta U^*)$ in (a); Left Dashed Line: $[\exp(-\Delta U^*)/W]f_W(\Delta U^*)$; Right Dashed Line: $f_W(\Delta U^*)/W$. (c) Solid Line: $f_{1/2}(\Delta U^*)$; Left Dashed Line: $f_{1/2}(\Delta U^*)\exp(-\Delta U^*/2)$; Right Dashed Line: $f_{1/2}(\Delta U^*)\exp(\Delta U^*/2)$. Left Scales are for Solid and Broken Lines, Right Scales are for Dashed Lines. The Horizontal Scale is the Same for All Figures

$$\equiv \frac{\langle g/W \rangle_W}{\langle 1/W \rangle_W} \tag{22}$$

where W is an arbitrary non-negative function, and $\langle\rangle_W$ denotes the average of a function weighted by $W\exp(-U_0/kT)$ (compared to the canonical ensemble average of a function which is weighted by $\exp(-U_0/kT)$). The integral introduced in the third step is a normalization factor.

In the Metropolis Monte Carlo calculation (see Chapter I), the acceptance or rejection of a trial move is determined by comparing the quantity, $[\exp(-U_0/kT)]_{new}/[\exp(-U_0/kT)]_{old}$, with a random number. Similarly, the average $\langle\rangle_W$ can also be obtained by a Monte Carlo method where the transition of a Monte Carlo step is determined by using the weighting function W, and comparing the quantity, $[W\exp(-U_0/kT)]_{new}/[W\exp(-U_0/kT)]_{old}$, with a random number. If in the modified Monte Carlo walk the number of steps falling between ΔU^* and $\Delta U^* + d\Delta U^*$ is denoted by $m_W(\Delta U^*)$, then similar to Equation (19), we can define a probability density function,

$$f_W(\Delta U^*) = \lim_{n\to\infty} m_W(\Delta U^*)/n \tag{23}$$

for the modified Monte Carlo walk. Equation (22) gives

$$\int g\, f(\Delta U^*)\, d\Delta U^* = \frac{\int (g/W)\, f_W(\Delta U^*)\, d\Delta U^*}{\langle 1/W \rangle_W} \tag{24}$$

Since the above equation holds for any function g, we obtain (20)

$$f(\Delta U^*) = \frac{f_W(\Delta U^*)/W}{\langle 1/W \rangle_W} \tag{25}$$

From Equation (22), we also have

$$\langle e^{-\Delta U^*} \rangle_0 = \frac{\int_{-\infty}^{\infty} \frac{e^{-\Delta U^*}}{W} f_W(\Delta U^*) d\Delta U^*}{\int_{-\infty}^{\infty} \frac{1}{W} f_W(\Delta U^*) d\Delta U^*} \tag{26}$$

Up to this point the function W has not been specified. One must choose this function to improve the accuracy of the simulation. But the detailed properties of the system being simulated are usually not known, so no general method for picking W exists. Torrie and Valleau (20) suggest that W be chosen by trial and error so that $f_W(\Delta U^*)$ is nearly uniform over a wide range. Because $\langle 1/W \rangle_W$ is independent of ΔU^*, Equation (25) gives $W \propto 1/f(\Delta U^*)$, if $f_W(\Delta U^*)$ is to be uniform over a wide range of energies. The shape of W as determined from $f(\Delta U^*)$ in Figure 3a is shown in Figure 3b. This shape is consistent with that obtained by Torrie and Valleau (20) who did not determine directly the $f(\Delta U^*)$, but tried to find a weighting function to make $f_W(\Delta U^*)$ uniform. In Figure 3b we see that the probability density for a Lennard-Jones system is appreciable at both of the important regions (around ΔU_L^* and ΔU_R^*, the regions where important contributions to numerator and denominator in Equation (26) occur). Thus, the Torrie-Valleau sampling is potentially much more efficient than the Metropolis Monte Carlo sampling for this system. The disadvantage, however, is that we have to spend time in finding an appropriate weighting function.

Half-Umbrella Sampling

Let us consider a specific choice for the weighting function,

$W = \exp(-\Delta U^*/2)$. Equation (26) becomes

$$\langle e^{-\Delta U^*} \rangle_0 = \frac{\int_{-\infty}^{\infty} e^{-\Delta U^*/2} f_{1/2}(\Delta U^*) d\Delta U^*}{\int_{-\infty}^{\infty} e^{\Delta U^*/2} f_{1/2}(\Delta U^*) d\Delta U^*} \qquad (27)$$

where $f_{1/2}(\Delta U^*)$ is the probability density function using $W = \exp(-\Delta U^*/2)$. The result is shown in Figure 3c. Again, $f_{1/2}(\Delta U^*)$ is of umbrella shape and its slope becomes steeper and steeper on both sides of ΔU^*_{mh} (the most probable position using $W = \exp(-\Delta U^*/2)$. In the Metropolis Monte Carlo walk, the most important contribution to Equation (18) occurs at the region around ΔU^*_{imp} where the rate of increase of $f(\Delta U^*)$ is roughly the same as the slope of $\exp(-\Delta U^*)$, while in the present sampling, the most important contributions to Equation (27) occur near the points, ΔU^*_N for the numerator and ΔU^*_D for the denomenator, where the slopes of $f_{1/2}(\Delta U^*)$ are roughly the same as those of $\exp(-\Delta U^*/2)$ and $\exp(\Delta U^*/2)$, respectively. Because the rate of change of $\exp(\pm\Delta U^*/2)$ is only one-half the rate of change of $\exp(-\Delta U^*)$, the distance between ΔU^*_{mh} and ΔU^*_N (or ΔU^*_D) should be smaller than the distance between ΔU^*_{mo} and ΔU^*_{imp}. Thus, $f_{1/2}(\Delta U^*_N)$ and $f_{1/2}(\Delta U^*_D)$ should be greater than $f(\Delta U_{imp})$. The sampling efficiency is then substantially increased. Figure 4 shows typical behavior of the Monte Carlo sampling using $W = 1$ (Metropolis) and $W = \exp(-\Delta U^*/2)$.

The above arguments apply for the cases that the slopes of $f(\Delta U^*)$ or $f_{1/2}(\Delta U^*)$ becomes steeper and steeper on both sides of the most probable position. This seems to be a general property for most systems. Otherwise, there would be an infinite range of ΔU^* which we have to sample. At any rate, we found that the surface excess free energy of water also has this property.

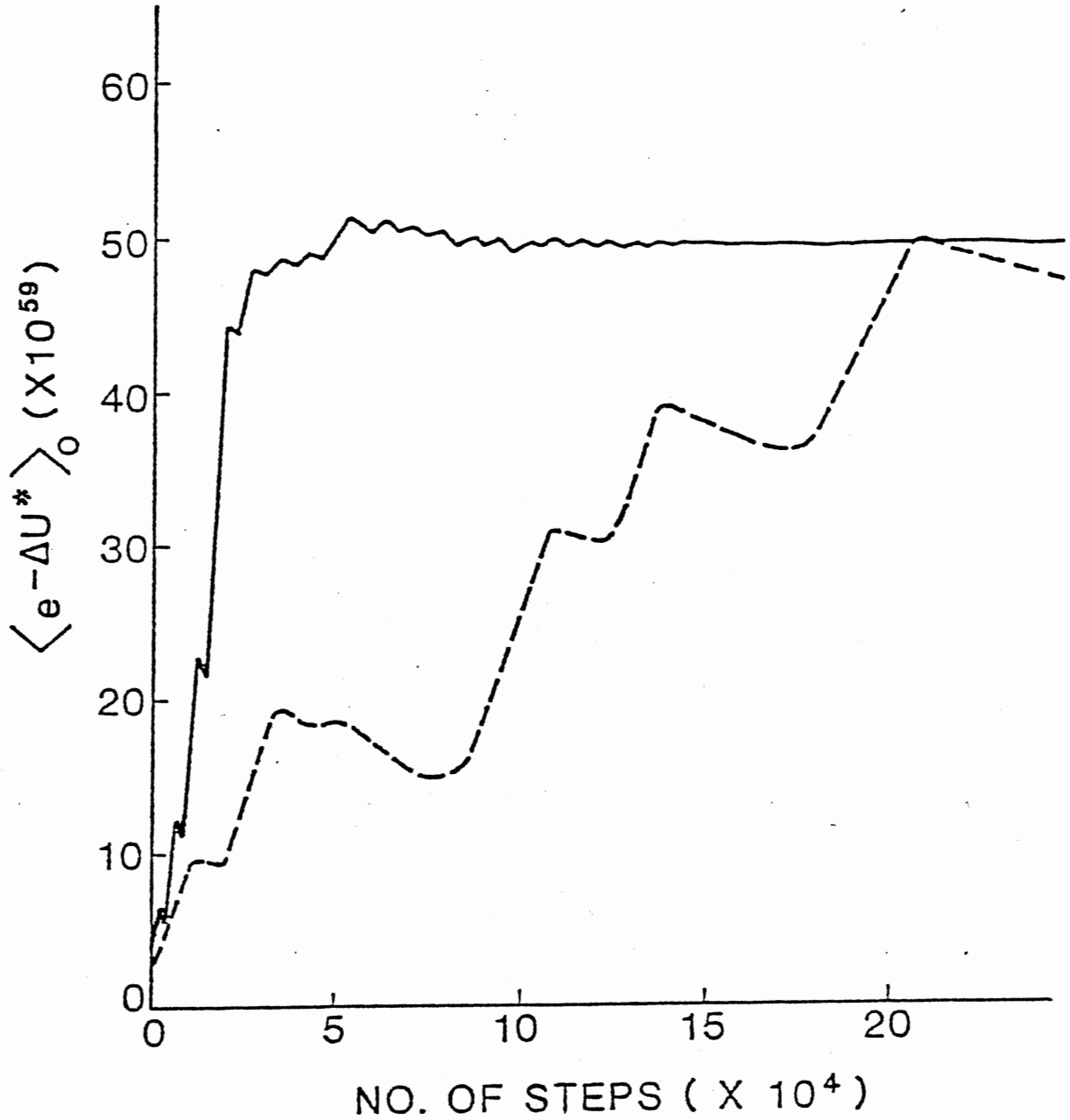

Figure 4. Behavior of Monte Carlo Samplings. Dashed Line Represents the Metropolis Monte Carlo Sampling and Solid Line Represents the Half-Umbrella Sampling. Both Start From a Configuration With ΔU^* Around the Most Probable Position, ΔU^*_{mo}, of the Metropolis Monte Carlo Walk

CHAPTER III

PROCEDURE FOR THE CALCULATION OF THE SURFACE TENSION

Outline of the Procedure

In Chapter II we presented a more efficient algorithm than the traditional Monte Carlo method to calculate the free energy difference between two systems using Equation (5). However, we note that Equation (5) is applicable only when the potential energies of both systems can be obtained from any configuration of one of the two systems. For the calculation of surface tension, according to Equation (3),

$$\gamma = (F_S - F_B)/A \tag{28}$$

where A is the total surface area, F_B represents the free energy of the bulk liquid and F_S denotes the free energy of the liquid with a surface. In a real liquid the potential energies of both states, "B" and "S" contains long range interactions which cannot be included in a practical computer simulation. Moreover, even if the long range interactions can be neglected, the potential energy of the state "S" is very difficult to be obtained from a configuration of the state "B". For these two reasons, Equation (5) cannot be applied directly to calculate $F_S - F_B$. Recently, Miyazaki et al. (15) proposed a procedure which involves Monte Carlo simulation of several intermediate states, computing the free

energy difference between each successive pair of states. We shall follow the same idea and use the following successive states:

(a) a bulk liquid with a nontruncated intermolecular potential;

(b) a bulk liquid using a truncated intermolecular potential;

(c) a slab shaped liquid with two hard-wall surfaces, using a truncated potential;

(d) a slab shaped liquid with two free surfaces using a truncated potential;

(e) a slab shaped liquid with two free surfaces using a nontruncated potential.

The procedure of Miyazaki et al. (15) also involves an intermediate state where the cutoff distance is increased to maintain the bulk density near the center of the slab when the hard walls are released. This state was omitted in our procedure because, as we shall see later, only about 2% of the molecules flow out of the surface. The density change at the slab center should be even smaller. The surface tension becomes

$$\gamma = (F_e - F_a)/2A$$

$$= \frac{1}{2A}\left[(F_e - F_d) + (F_d - F_c) + (F_c - F_b) + (F_b - F_a)\right] \qquad (29)$$

In the following sections, we consider each of the terms in Equation (29) separately.

The Main Contribution: $F_c - F_b$

The term, $F_c - F_b$, represents the free energy change in separating the slab shaped liquids. During the separation process, the potential energy of this system can be described by a modified potential, making

use of periodic boundary conditions (see Figure 5),

$$U = \sum_{i<j=1}^{N} \sum_{\ell,m,n=-1}^{1} u\{[(x_i - x_j + \ell L_x)^2 + (y_i - y_j + mL_y)^2 + (z_i - z_j + nL_z + nd)^2]^{1/2}\} \quad (30)$$

where L_x, L_y, and L_z represent the size of the unit cell, and u(r) denotes the pair potential function in which the interaction is neglected when the distance of two molecules is greater than a cutoff distance, R_c. The summation over ℓ, m and n from -1 to 1 contains 27 terms, which corresponds to one "central" unit cell and 26 nearest-neighbor cells. That is, in the calculation of the interaction energies between a given molecule i and its surrounding molecules, another molecule j in the central unit cell has 26 images. All of the 27 "j-th" molecules may be included in the sphere of radius R_c surrounding the i-th molecule. However, if R_c is less than half of the side-length of the unit cell, only the one closest to i may not be neglected. This choice is referred to as the "minimum image convention" (21). In our computer program, the distance between the i-th molecule and its closest j-th molecule is determined by a subroutine DIST (see Appendix C). The parameter d represents the separation between two slabs. When $d = R_c$, the slabs are completely separated, and when d = 0, Equation (30) reduces to the potential energy of the state (b). Thus, from Equation (5) we have

$$F_c - F_b = - kT \ln \langle e^{-\Delta U^*_{bc}} \rangle_b \quad (31)$$

where

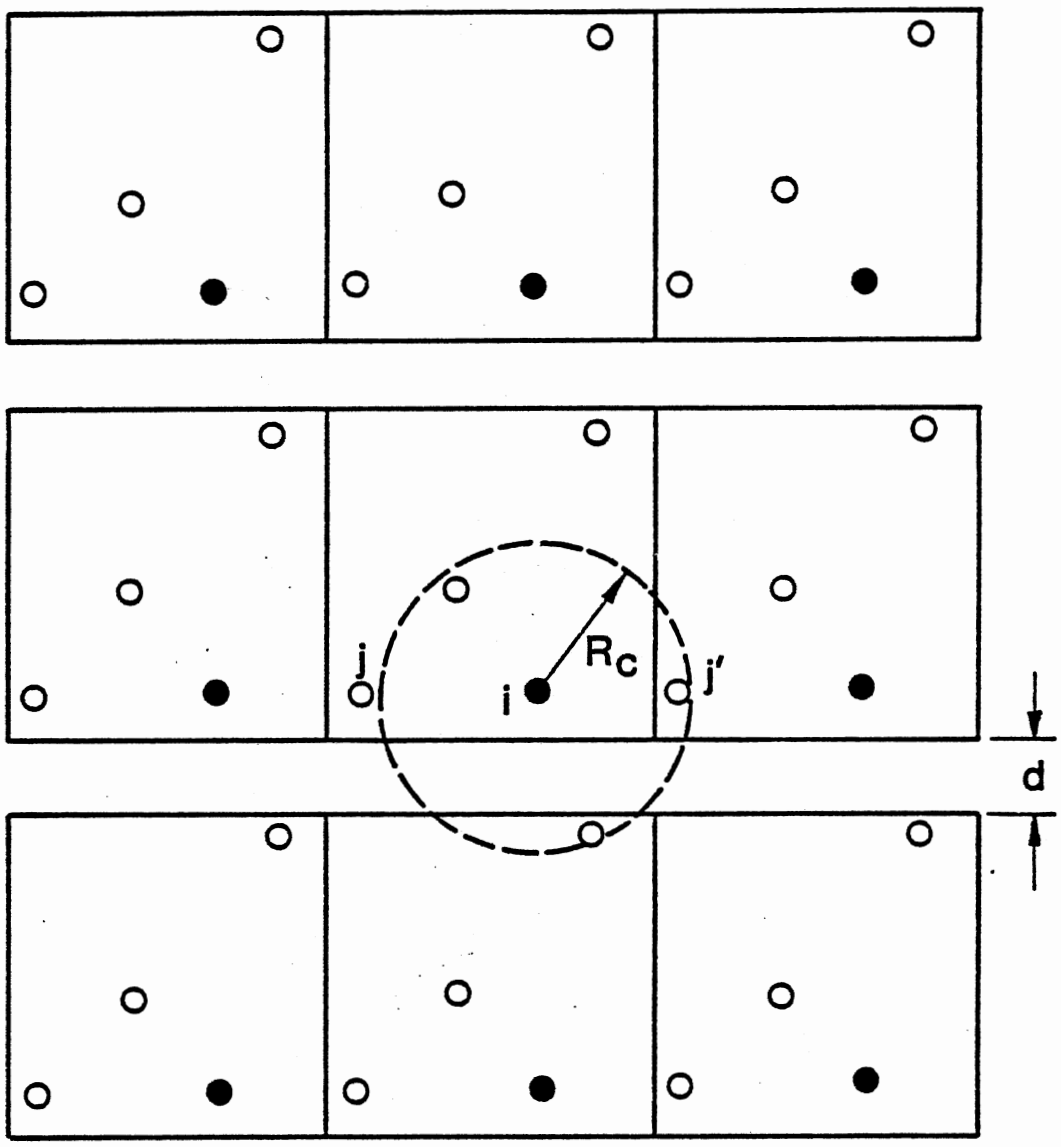

Figure 5. The Modified Periodic Boundary Conditions

$$\Delta U^{*}_{bc} = \frac{1}{kT}\left[U(d = R_c) - U(d = 0)\right] . \qquad (32)$$

$F_c - F_b$ can also be viewed as the work required to separate the slabs. If R_c is large enough, this term should have the major contribution to the total surface tension.

Contribution From Long-Range Interactions

The term, $F_a - F_b$, arises from the interactions between each molecule i and the molecules outside the sphere of radius R_c surrounding the i-th molecule. It is composed of two parts: (i) the free energy required to polarize the medium outside the sphere, and (ii) the energy $-\vec{\mu}_i \cdot \vec{B}_i$ of the i-th molecule (with dipole moment $\vec{\mu}_i$) in the reaction field $\vec{B}_i$ which is produced by the medium polarized by the i-th molecule (22). The first part is proportional to B_i^2, say CB_i^2 (22). Then for each molecule the long-range contribution is

$$\Delta F^{i}_{LR} = -\vec{\mu}_i \cdot \vec{B}_i + C\, B_i^2 \qquad (33)$$

To find C, we use the fact that for a system in equilibrium the free energy should be a minimum, and consider that ΔF^{i}_{LR} depends on B_x, B_y, and B_z,

$$\frac{\partial \Delta F^{i}_{LR}}{\partial B_{ix}} = 0, \quad \frac{\partial \Delta F^{i}_{LR}}{\partial B_{iy}} = 0, \quad \frac{\partial \Delta F^{i}_{LR}}{\partial B_{iz}} = 0 \qquad (34)$$

which gives

$$2\, C\, \vec{B}_i = \vec{\mu}_i \qquad (35)$$

Inserting this into Equation (33),

$$\Delta F^{i}_{LR} = -\vec{\mu}_i \cdot \vec{B}_i + \frac{1}{2}\vec{\mu}_i \cdot \vec{B}_i = -\frac{1}{2}\vec{\mu}_i \cdot \vec{B}_i \tag{36}$$

The reaction field can be obtained by solving the Laplace Equation (22),

$$\vec{B}_i = \frac{2(\varepsilon - 1)}{(2\varepsilon + 1)R_c^3}\vec{M}_i \tag{37}$$

where ε is the dielectric constant and $\vec{M}_i$ represents the net dipole moment in the sphere surrounding the i-th molecule. Therefore, in a system of canonical distribution of configurations,

$$F_b - F_a = -\sum_{i=1}^{N} \Delta F^{i}_{LR} = \frac{(\varepsilon - 1)}{(2\varepsilon + 1)R_c^3} < \sum_{i=1}^{N} \vec{\mu}_i \cdot \vec{M}_i >_b \tag{38}$$

The term, $F_e - F_d$, is due to the long-range interactions in a liquid with surface. Its value is very difficult to obtain accurately. As a rough estimate, we assume

$$F_e - F_d \approx \frac{2}{3}(F_a - F_b) \tag{39}$$

because the slab shaped liquid extends only in two dimensions. The error in this approximation may be potentially large. However, in Equation (38) the contribution of $F_b - F_a$ to the total surface tension is proportional to R_c^{-3}. Similarly, the contribution of $F_e - F_d$ should vary inversely with same power of R_c, so we can choose a large R_c to make the error of the total surface tension small.

Contribution From Relaxing the Hard Wall Constraint

To change the system from state (c) to state (d), we gradually increase the distance between two hard walls. Let t_1 and t_2 be the values of the z coordinate at which the walls are located (initially L_z and 0). The configuration integral of this system can be expressed by

$$Q = \int e^{-U/kT} \prod_i [H(t_1-z_i)H(z_i-t_2)]dq^N \tag{40}$$

where H(x) is the step function which is 0 for $x < 0$ and 1 for $x > 0$; the derivative of H(x) is the Dirac delta function, $\delta(x)$. Then

$$\frac{\partial \ln Q}{\partial t_1} = \frac{\int e^{-U/kT}[\Sigma\, \delta(t_1-z_i)/H(t_1-z_i)]\pi[H(t_1-z_i)H(z_i-t_2)]dq^N}{Q}$$

$$= \langle \Sigma\, \delta(t_1-z_i)/H(t_1-z_i)\rangle \tag{41}$$

At this stage the step function in Equation (41) can be omitted, since the z-components of all molecules are less than t_1 and thus $H(t_1-z_i)$ is equal to unity. Integrating Equation (41),

$$\int_{L_z}^{\infty} \frac{\partial \ln Q}{\partial t_1} dt_1 = \int_{L_z}^{\infty} \langle \Sigma\, \delta(t_1-z_i)\rangle dt_1 \tag{42}$$

Let Q_i and Q_f be the configuration integrals for the system before and after relaxation of one surface, respectively. The free energy difference due to the relaxation per surface is

$$\Delta F_{if} = - kT \ln(Q_f/Q_i)$$

$$= - kT \int_{L_z}^{\infty} <\Sigma \delta(t_1 - z_i)> dt_1 \qquad (43)$$

Equation (43) was first obtained by Miyazaki et al. (15). From this equation, it is clear that

$$F_d - F_c = - kT\{\int_{L_z}^{\infty} <\sum_i \delta(t - z_i)> dt + \int_{-\infty}^{0} <\sum_i \delta(t - z_i)> dt\}$$

$$= - kT <N_{out}> \qquad (44)$$

where N_{out} represents the number of molecules which move out of the two surfaces after the two walls are released.

CHAPTER IV

COMPUTATIONAL DETAILS

According to the procedure described in Chapter III, a surface tension calculation should involve three canonical ensemble averages, $\langle \exp(-\Delta U^{*}_{bc}) \rangle_b$, $\langle \Sigma \vec{\mu}_i \cdot \vec{M}_i \rangle_b$, and $\langle N_{out} \rangle$ in Equations (31), (38), and (44) respectively. The first one can be evaluated by the half-umbrella sampling algorithm as described in Chapter II, and the last two are suitable for the Metropolis Monte Carlo method since they contain no rapidly varying functions. The general procedure for the Metropolis algorithm has been given in the Introduction. Figure 6 shows the flow chart of the half-umbrella sampling. In the following sections we describe our computation in more detail.

Initial Configuration

As mentioned earlier, the cutoff distance R_c should be sufficiently large to reduce the long range error made by Equation (39). On the other hand, by the minimum image convention (see Chapter III), the length of the unit cell should be greater than $2R_c$. In our simulation model, R_c is chosen to be 9.8Å, which is about half of the length, 19.72Å, of our cubic unit cell containing 256 water molecules. The density of water is then equal to 1 g/cm^3. In this study, the ST2 potential will be used. Because neither the ST2 nor the CI potentials can accurately reproduce the internal energy of water (see the Introduc-

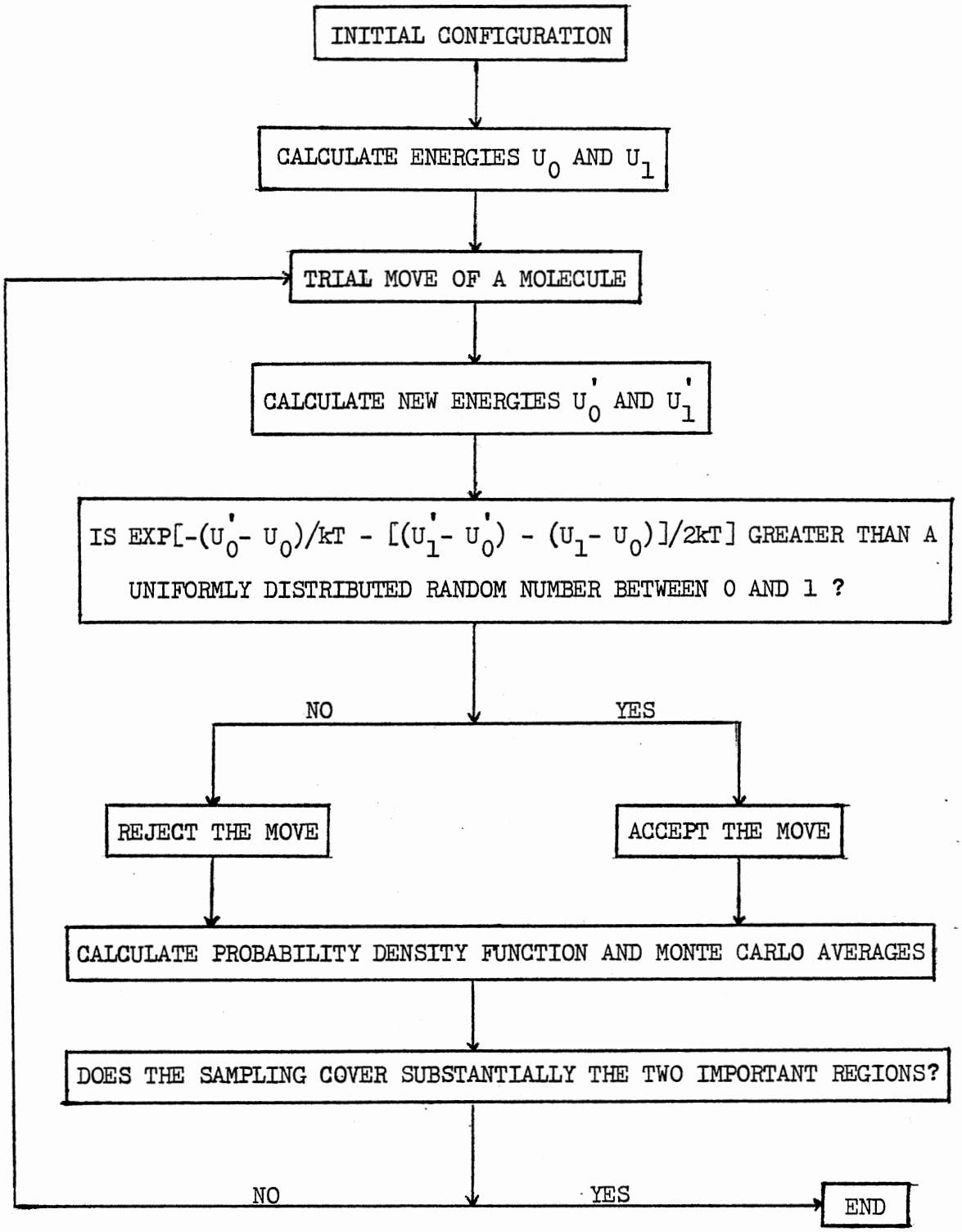

Figure 6. Flow Chart of the Half-Umbrella Sampling

tion), there is no reason to favor one potential over the other for the computation of the surface tension. We chose the ST2 potential because it is simpler and requires less computer time to work with.

The ST2 water molecule can be specified by three Cartesian coordinates (x,y,z) for the center of the molecule and three Euler angles (θ,ψ,α) for the rotational position about the center. The normal to the water surface is taken to be the z-axis. θ and ψ denote the spherical polar and azimuthal angles of the dipole moment (pointing from the center to the middle point of the two positive charges). α represents the rotational angle of the molecule about the dipolar axis. The initial positions of all of the 256 molecules in a unit cell are chosen randomly using the random number algorithm RANF written by Dr. J. P. Chandler of the OSU computer science department.

Calculation of Potential Energy

Equation (30) is a general expression for the potential energy of the systems in which we are interested. As mentioned earlier, the distance between the molecular centers is calculated by the subroutine DIST (see Appendix C). When the ST2 potential, Equation (12), is used, we have to calculate the distance between charges of two different molecules. For this purpose, we need to know their coordinates in the laboratory frame. Let O'Z' denote the dipolar axis (O' being the center of the ST2 molecule), O'X' represent the axis perpendicular to O'Z' and to the face ABCD of the cube determined by the ST2 water model (see Figure 7), and O'Y' be the third axis perpendicular to both O'X' and O'Z'. In this body frame, the coordinates of the m-th charge of each molecule is given by

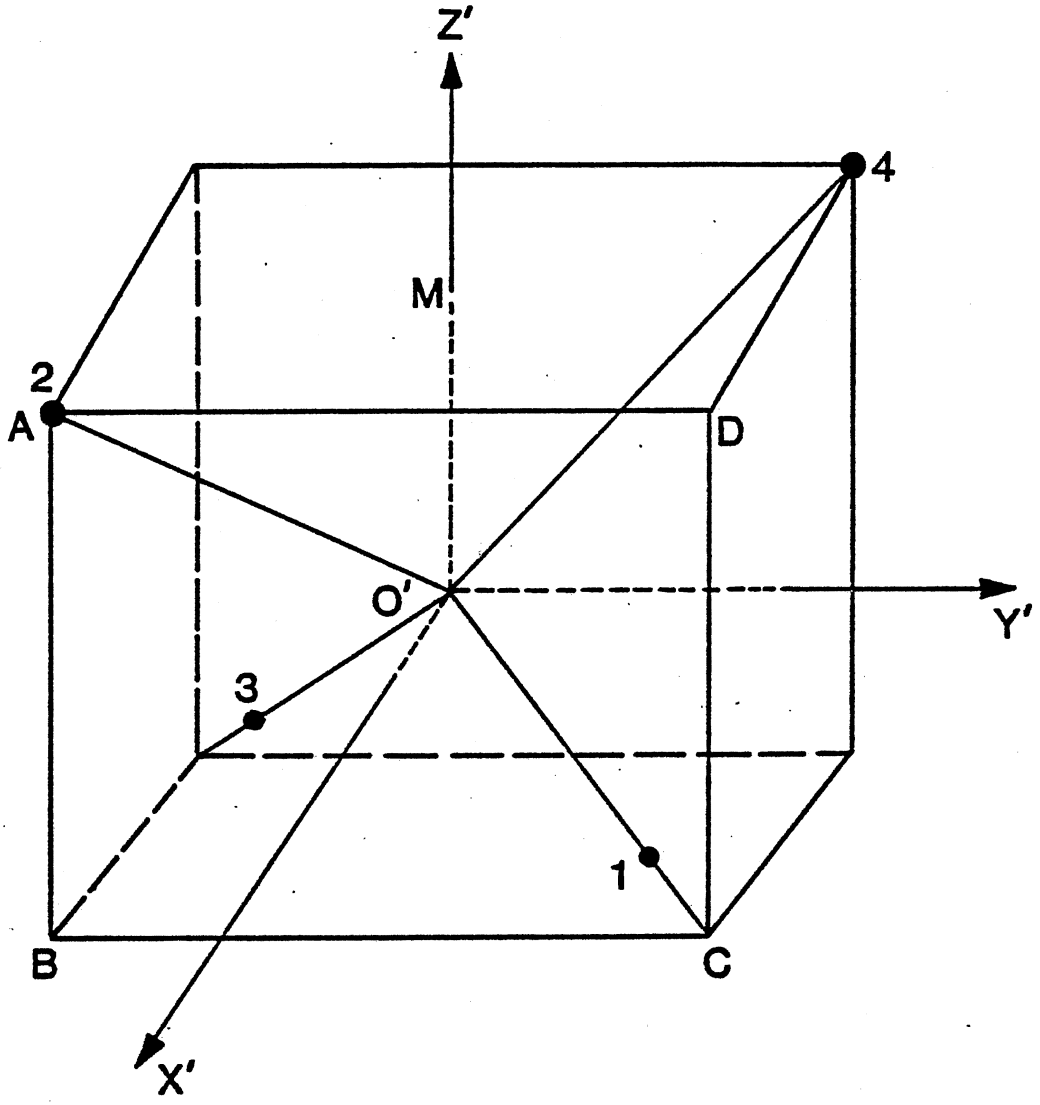

Figure 7. Definition of the Body Frame for the ST2 Water Molecule

$$CX(1) = 0.8\, d_{O'M} \qquad CY(1) = 0.8\, d_{O'M} \qquad CZ(1) = -0.8\, d_{O'M}$$

$$CX(2) = d_{O'M} \qquad CY(2) = -d_{O'M} \qquad CZ(2) = d_{O'M}$$

$$CX(3) = -0.8\, d_{O'M} \qquad CY(3) = -0.8\, d_{O'M} \qquad CZ(3) = -0.8\, d_{O'M}$$

$$CS(4) = -d_{O'M} \qquad CY(4) = d_{O'M} \qquad CZ(4) = d_{O'M}$$

where

$$d_{O'M} = \cos(\theta_t/2) = 0.57735$$

In the laboratory frame, the coordinates of the m-th charge of i-th molecule become (23)

$$\vec{A}(m,i) = D_z(\psi_i)\, D_y(\theta_i)\, D_z(\alpha_i)\, \vec{C}(m) \tag{45}$$

where

$$D_z(\psi_i) = \begin{pmatrix} \cos\psi_i & -\sin\psi_i & 0 \\ \sin\psi_i & \cos\psi_i & 0 \\ 0 & 0 & 1 \end{pmatrix}$$

$$D_y(\theta_i) = \begin{pmatrix} \cos\theta_i & 0 & \sin\theta_i \\ 0 & 1 & 0 \\ -\sin\theta_i & 0 & \cos\theta_i \end{pmatrix}$$

$$D_z(\alpha_i) = \begin{pmatrix} \cos\alpha_i & -\sin\alpha_i & 0 \\ \sin\alpha_i & \cos\alpha_i & 0 \\ 0 & 0 & 1 \end{pmatrix}$$

Then the distance, $d_{mn}(i,j)$, in Equation (13) is given by

$$d_{mn}(i,j) = \left|\vec{r}_i + \vec{A}(m,i) - \vec{r}_j - \vec{A}(n,j)\right| \tag{46}$$

where $\vec{r}_i$ and $\vec{r}_j$ represent the positions of the molecular centers.

Trial Move of a Molecule

At each Monte Carlo step, a molecule is moved according to $q_j \rightarrow q_j + \xi_j \delta q_j$, where q_j is the j-th coordinate (= x,y,z,θ,ψ, or α) of the molecule, δq_j is the maximum allowed displacement and ξ_j is a random number uniformly distributed between -1 and 1. The value of δq_j is essential for the speed with which the system approaches equilibrium. As mentioned in the Introduction, its value is usually chosen so that about half of the trial moves are accepted. For the ST2 water, we choose $\delta x = \delta y = \delta z = 0.13\text{Å}$ and $\delta\theta = \delta\psi = \delta\alpha = 0.13$ radian. The acceptance probability is close to 50% either using the Metropolis sampling or the half-umbrella sampling.

Acceptance or Rejection of the Trial Move

In the general umbrella sampling algorithm (see Chapter II), the acceptance or rejection of a trial move is determined by comparing the ratio $[W\exp(-U_0/kT)]_{new}/[W\exp(-U_0/kT)]_{old}$, with a random number uniformly distributed between 0 and 1, where W is an arbitrary weighting function. If the ratio is greater than the random number, the trial move is accepted; otherwise, it is rejected. We see that the umbrella sampling reduces to the Metropolis sampling when W = 1. In the calculation of $\langle\exp(-\Delta U^*)\rangle_0$, we use $W = \exp(-\Delta U^*/2)$ (called half-umbrella

sampling), since it gives better efficiency than the Metropolis sampling as shown in Chapter II.

Location of the Important Regions

From Chapter II, it is clear that the accuracy of the Monte Carlo sampling algorithm depends on whether the two important regions of configuration space (the most important contributions to the denominator and numerator of Equation (27)) are covered or not. In Chapter II, the location of the two important regions for the Lennard-Jones system were found by a direct search of the configuration space over a certain range of ΔU^* which should cover the two important regions. However, if the two important regions are quite far apart in energy ΔU^*, this method will require a large number of steps. A much more efficient way is suggested as follows.

From Equation (25), because $\langle 1/W \rangle_w$ is independent of ΔU^*, one can obtain

$$\frac{f_W(\Delta U^*)}{W} \propto f(\Delta U^*) \tag{47}$$

$$\frac{e^{-\Delta U^*}}{W} f_W(\Delta U^*) \propto f(\Delta U^*) e^{-\Delta U^*} \propto f_1(\Delta U^*) \tag{48}$$

where $f_1(\Delta U^*)$ is the probability density function using $W = \exp(-\Delta U^*)$. Thus, the important regions for the denominator and numerator of Equation (27) should be around the maxima of $f(\Delta U^*)$ and $f_1(\Delta U^*)$, respectively. This result is true for any weighting function. The distance between the two maxima will be called the "important range", which is

an intrinsic property of a given system. Since the Monte Carlo walk concentrates on the maximum of a probability density function, to find the maxima of $f(\Delta U^*)$ and $f_1(\Delta U^*)$ is obviously much more efficient than to determine the probability density function over a wide range of ΔU^*.

The probability density function is defined to be $m(\Delta U^*)/n$, where n is the total number of Monte Carlo steps, $m(\Delta U^*)$ denotes the number of steps falling between ΔU^* and $\Delta U^* + d\Delta U^*$. In this study, a certain range of ΔU^* is divided into many small regions and the width of each region, $d\Delta U^*$, is chosen to be 1 (in unit kT). At each step, we determine the i-th region to which the ΔU^* of that step belongs. $m(\Delta U^*)$ can be obtained by counting the number of steps falling into the i-th region.

For more details on the computer calculation, one is referred to Appendix C.

CHAPTER V

MODEL SYSTEMS STUDIED AND THEIR RESULTS

Air-Water Interfaces

The Main Contribution $F_c - F_b$

Using the method given in the last section of the previous chapter, we find that the important range (distance between two important regions) for $F_c - F_b$ is more than 300 (in unit kT), which is about 40 times the important range of the free energy difference for the simpler system studied in Chapter II. In this case, the Torrie-Valleau method involving a search for an appropriate weighting function to make $f_W(\Delta U^*)$ nearly uniform is extremely tedious and requires a large number of steps. For the half-umbrella sampling, as shown below, the probability density at the two important regions, around ΔU_N^* and ΔU_D^*, also becomes very small. From Chapter II, we can see that $f_{1/2}(\Delta U_N^* + 0.5)/f_{1/2}(\Delta U_N^* - 0.5)$ $\sim f_{1/2}(\Delta U_D^* - 0.5)/f_{1/2}(\Delta U_D^* + 0.5) \sim \exp(1/2)$, and $f_{1/2}(\Delta U_{mh}^* + 0.5)/f_{1/2}(\Delta U_{mh}^* - 0.5) \sim 1$ where ΔU_{mh}^* locates the peak in $f_{1/2}$ itself. For a rough estimate of the relative sizes of the distributions we assume that the slope (on a logarithmic scale) of $f_{1/2}(\Delta U^*)$ changes uniformly from ΔU_{mh}^* to ΔU_N^* or ΔU_D^*. Then a simple geometric argument gives $f_{1/2}(\Delta U_D^*) \sim f_{1/2}(\Delta U_N^*) \sim 10^{-16} f_{1/2}(\Delta U_{mh}^*)$ if the range in ΔU^* is 300 from ΔU_N^* to ΔU_D^*.

The above argument shows that the probability density at the two important regions increases rapidly with decreasing values of $\Delta U_D^* - \Delta U_N^*$. For this reason, we make this range smaller by dividing $F_c - F_b$ into several stages, and doing m computer runs instead of one very long run. That is, we write

$$F_c - F_b = \sum_{j=0}^{m} (F_{j+1} - F_j)$$

$$= - kT\{\sum_{j=0}^{m} \ln\langle e^{-\Delta U_j^*}\rangle_j\} . \qquad (49)$$

where $\Delta U_j^* \equiv [U(d_{j+1}) - U(d_j)]/kT$ and $\langle\rangle_j$ denotes the canonical average over the configurations of the slab shaped liquid with separation $d_j (d_o \equiv 0;\ d_{m+1} \equiv R_c)$. For each stage, 1.5×10^5 steps were generated. The probability density function was found to be very similar to that given in Chapter II, i.e., the slope of $f_{1/2}(\Delta U_j^*)$ becomes steeper and steeper on both sides of the most probable region. The canonical average and the important range for each stage are given in Table I for $T = 298^{\circ}K$. From these results, we have $F_c - F_b = 108 \pm 5$ kcal/mole. This gives a contribution to the surface tension of 96.5 ± 4.5 dynes/cm.

The Long Range Contribution

The long range contribution can be obtained from Equations (38) and (39). The dielectric constant of water is known to be 78.5 (24). Although the ST2 potential may not give the same value, we can still use the experimental value for ε in Equation (38), since $F_b - F_a$ is very insensitive to the dielectric constant when it is large. For the ST2 molecule, $\mu = 2.353$ debye. The canonical ensemble average, $\langle\Sigma\vec{\mu}_i \cdot \vec{M}_i\rangle_b$

TABLE I

FREE ENERGY DIFFERENCES AND IMPORTANT RANGES IN ENERGY AS A FUNCTION OF THE SEPARATION DISTANCE BETWEEN SLABS

Separation d_j (Å)		$\ell n \langle e^{-\Delta U_J^*} \rangle_j$	$\Delta U_D^* - \Delta U_N^*$
From	To		
0	0.15	- 0.1 ± 0.2	20
0.15	0.3	- 0.7 ± 0.6	20
0.3	0.5	- 5.3 ± 0.5	20
0.5	0.7	- 5.5 ± 0.5	20
0.7	0.9	- 7.6 ± 0.8	30
0.9	1.1	- 5.3 ± 0.5	20
1.1	1.35	-13.8 ± 1.5	40
1.35	1.5	- 8.2 ± 0.6	20
1.5	1.7	-10.0 ± 0.8	25
1.7	1.9	-10.4 ± 0.8	25
1.9	2.1	-17.3 ± 0.5	20
2.1	2.3	-11.7 ± 0.5	20
2.3	2.5	-15.4 ± 0.5	20
2.5	3.2	-41.6 ± 0.4	20
3.2	9.8	-29.5 ± 0.2	10

can be obtained by a conventional Monte Carlo calculation. From Equation (38), we have $F_b - F_a = 12.5 \pm 0.5$ kcal/mole which, with the surface area chosen, corresponds to a contribution to γ of 11 ± 0.45 dyne/cm. Then Equation (39) gives $(F_b - F_a) + (F_e - F_d) \approx 3.7$ dyne/cm. The error of this result is estimated to be less than 1 dyne/cm, assuming Equation (39) is accurate to within 25%.

The Relaxation Contribution $F_d - F_c$

Recall that this free energy difference is proportional to the number of molecules which leave the system via the surface, $\langle N_{out} \rangle$. To calculate $\langle N_{out} \rangle_d$, we first equilibrate the state (c). Then, in the subsequent Monte Carlo walk, the two hard walls are released, corresponding to the state (d). In this calculation, the conventional Monte Carlo method is used. After 10^5 steps, we find $\langle N_{out} \rangle_d = 5.6 \pm 0.4$. Equation (44) gives $F_d - F_c = -3.3 \pm 0.2$ kcal/mole. This gives a contribution to the surface tension of -2.9 ± 0.2 dynes/cm.

Combining the results in (A), (B), and (C), we finally obtain $\gamma = 97 \pm 6$ dyne/cm, for $T = 298^{\circ}K$. The experimental value at this temperature is 72 dyne/cm (25). Reasons for the discrepancy will be discussed in Chapter VI.

Lipid-Water Interfaces

Lipids are the building blocks of cell membranes. They are amphiphilic molecules containing a polar head group and a non-polar portion consisting of hydrocarbon chains. When lipids are spread at air-water interface at areas of less then 100Å^2 per molecule, a monolayer of well-aligned lipid molecules are formed. The hydrophilic polar group is

anchored at the interface with its dipole moment parallel to the surface (26) and the hydrocarbon chains project out of the water and associated with each other (Figure 8). The free energy of the lipid-water interface should depend on the following interactions: head group-water, chain-chain, chain-air, chain-water, and head group-chain. The last two interactions, however, are unlikely to depend on the molecular area (27,28). Thus, the surface tension of the lipid-water interface can be written

$$\gamma_{LW} \equiv \frac{\partial F}{\partial A} = \gamma_{hw} - \pi_{cc} + \gamma_{ca} \qquad (50)$$

where γ_{hw} is the surface tension of the head group-water interface, π_{cc} is the chain pressure due to closely packed but not frozen chains, and γ_{ca} is the surface tension of the chain-air interface. The thermodynamic properties of the hydrocarbon chains have been extensively studied by theoreticians (29). However, the head group-water interface is far less understood. In this section, we shall apply the previous method to calculate the term, γ_{hw}. Then, using the theoretical results of π_{cc} and γ_{ca}, we can compare our results with the experimental values of γ_{LW}.

Phosphatidylcholine is one of the commonly observed lipids in nature. Its head group is shown in Figure 9. We note that there is a positive charge at the N atom and a negative charge at the P atom. Since electrostatic force is the dominate force in our system, it is reasonable to approximate the head group-head group and head group-water interactions by dipole-dipole interactions. The dipole moment of the head group is about 20 debyes as estimated from the distance between P and N atoms. However, because the dipolar field produced by the head

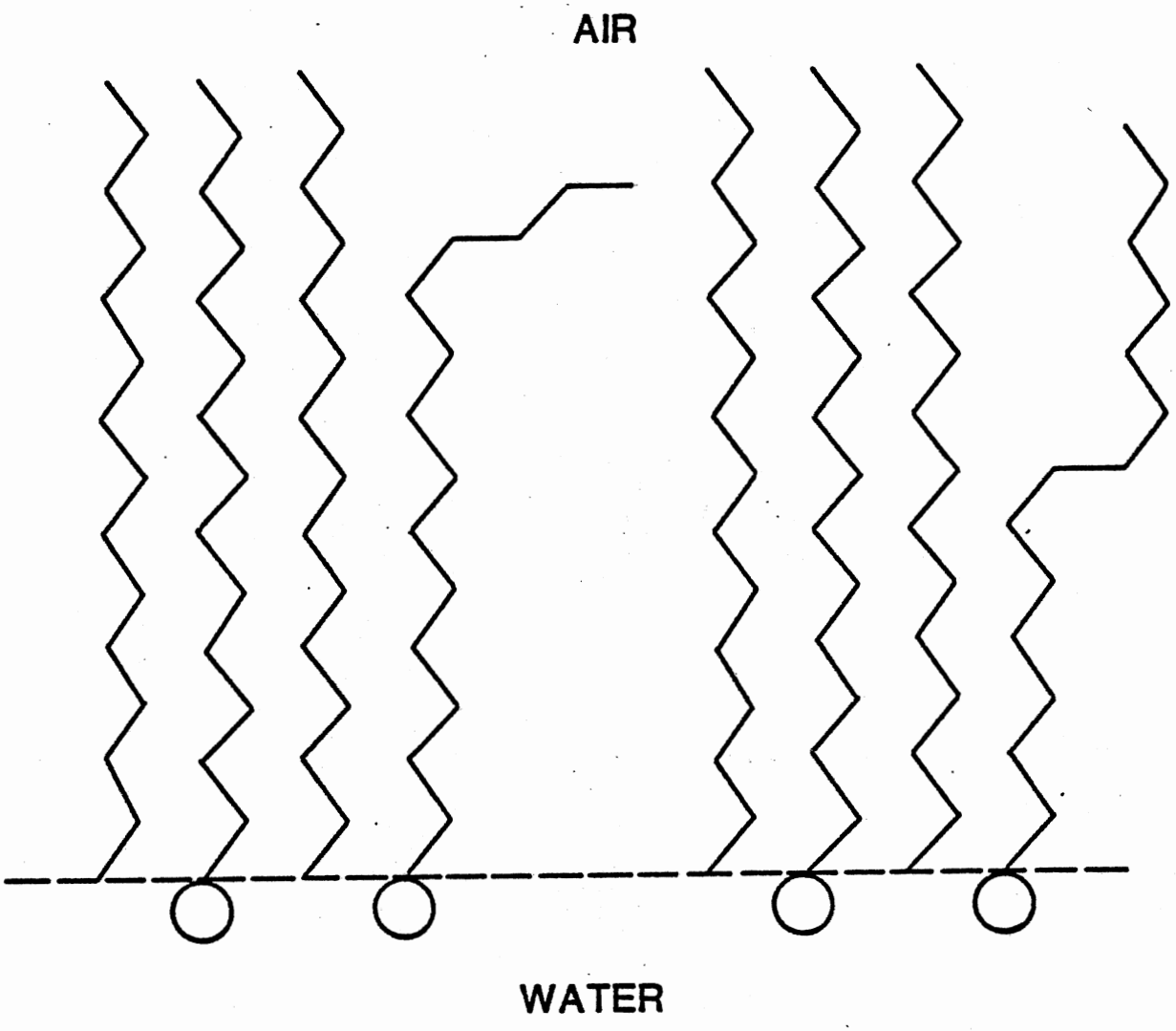

Figure 8. Schematic Representation of the Lipids Spreading at Air/ Water Interface. The Zig-Zag Lines Represent the Hydrocarbon Chains and the Circles Represent Head Groups

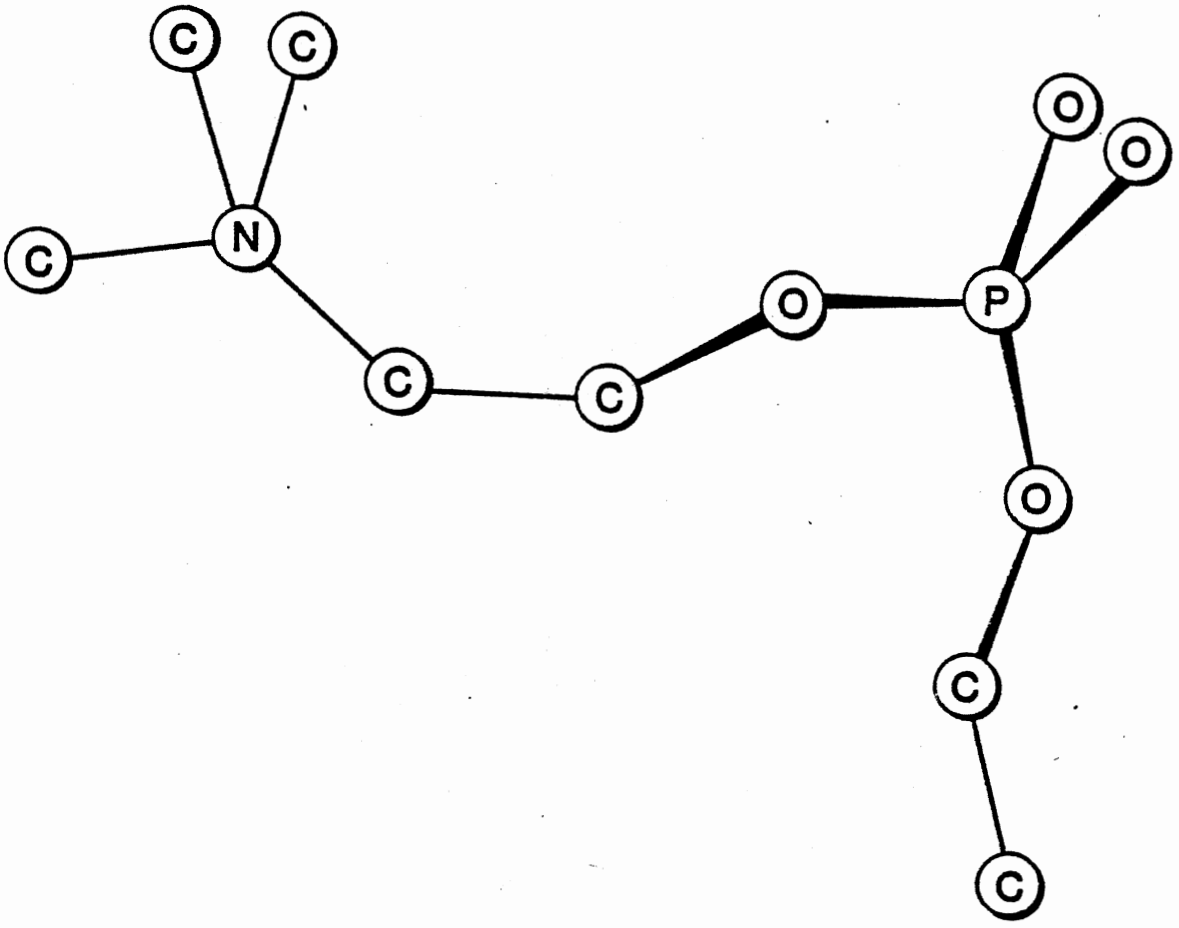

Figure 9. The Head Group of Phosphatidylcholine

group can be shielded by its medium (e.g., water), the effective dipole moment of the head group should be smaller. In a continuous medium of dielectric constant ε, it is reduced by a factor of ε. In our procedure of calculating the surface tension, the modified periodic boundary conditions as shown in Figure 5 are used. In this system, the effective dipole moment is very difficult to estimate. For this reason, we have calculated the surface tension under a variety of circumstances. Figure 10 shows schematically the systems studied. In each case our system consisted of eight head groups and 248 water molecules. The density of the head groups was chosen to be 50Å^2/head group. In the surface layer, the top 5Å, the head group dipoles are held fixed, but can flip-flop in their orientation, while the water in this top layer is allowed to rotate freely and to move perpendicular to the surface, but not laterally in the plane of the surface. These restrictions are realistic from a steric point of view.

We studied five different systems. Four of the systems had one free water per head group and varying head group dipole strengths, while the fifth system had no free water in the surface layer. From the previous results on pure water, we see that the long range contribution and the relaxation contribution are about to cancel. For this reason, we calculate only the main contribution $F_c - F_b$. The results are presented in Table II. For the system with a large surface dipole moment but no free surface water (run 1), the surface tension is smallest, while insertion of one free water into the surface (runs 2-5) makes the surface tension considerably larger. This is because that each head group dipole has only two different configurations so that the free energy change (logarithm of the configuration integral) is small as the two slabs are

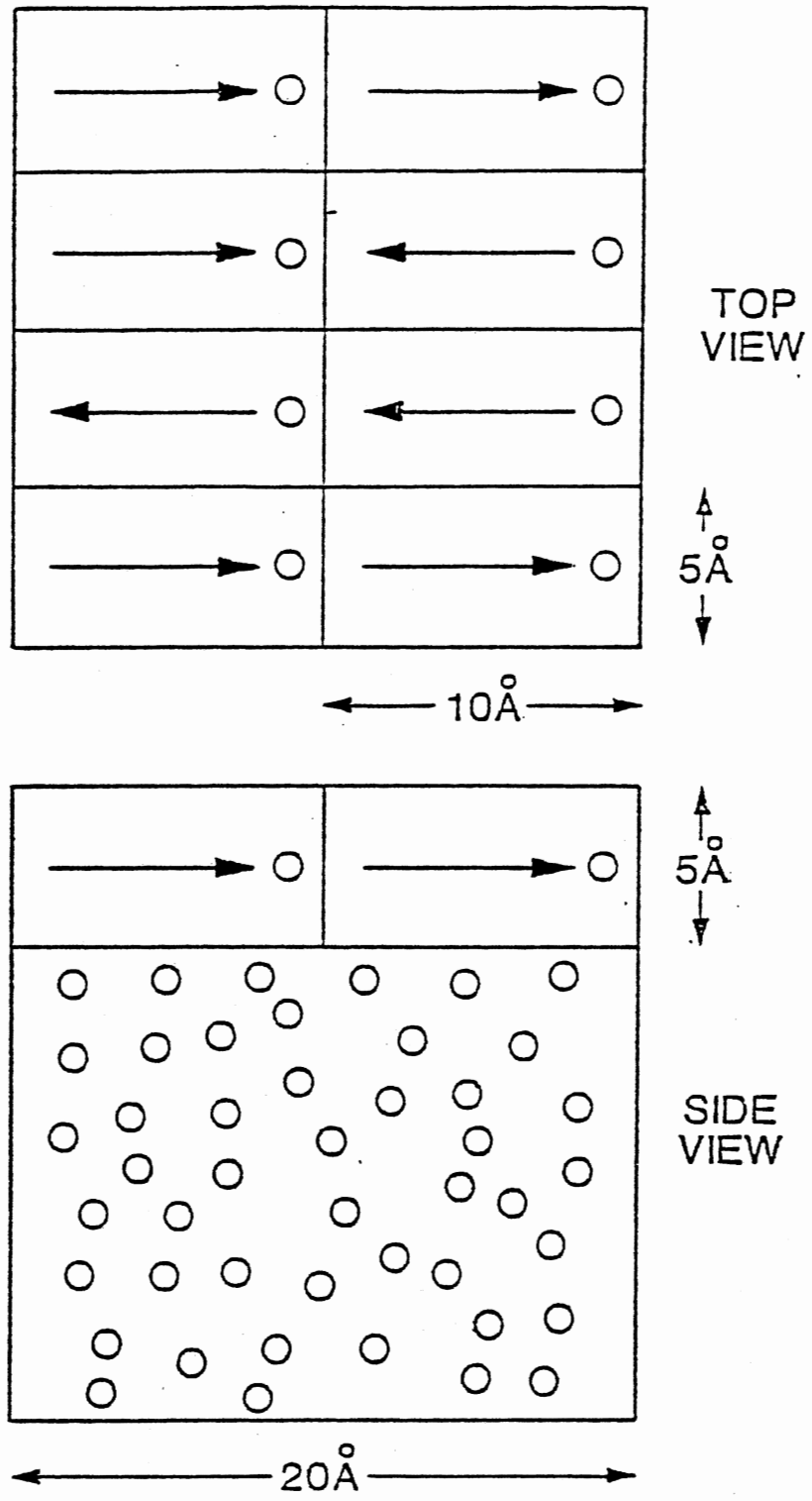

Figure 10. Top and Side Schematic Views of the Systems Simulated. The Arrows Represent Head Group Dipoles and the Circles Represent Water

TABLE II

SYSTEMS STUDIED AND RESULTING SURFACE TENSION VALUES

Run	Head Group Dipole Strength	Water/Lipid in Surface	Surface Tension[a]
1	20 Debye	0	32 dynes/cm
2	15 Debye	1	115 dynes/cm
3	10 Debye	1	82 dynes/cm
4	5 Debye	1	70 dynes/cm
5	1 Debye	1	45 dynes/cm

[a]The uncertainty in all cases is estimated to be ± 6 dynes/cm.

separated. With one free water per head group and with a head group dipole strength of 15 debyes, the surface tension is 115 ± 6 dynes/cm greater than the calculated value for pure water. This is because the total dipole strength is much greater than that of a pure water interface. Since the surface tension of a lipid/water interface is necessarily less than that of air/water interface we conclude that the effective head group dipole moment should be smaller than 15 debyes. In Figure 11, we plot the ratio of the calculated surface tension to the calculated air/water surface tension, 97 dynes/cm, against dipole strength for runs 2-5 (Table II). The line is a least squares fit to the midpoints of the data.

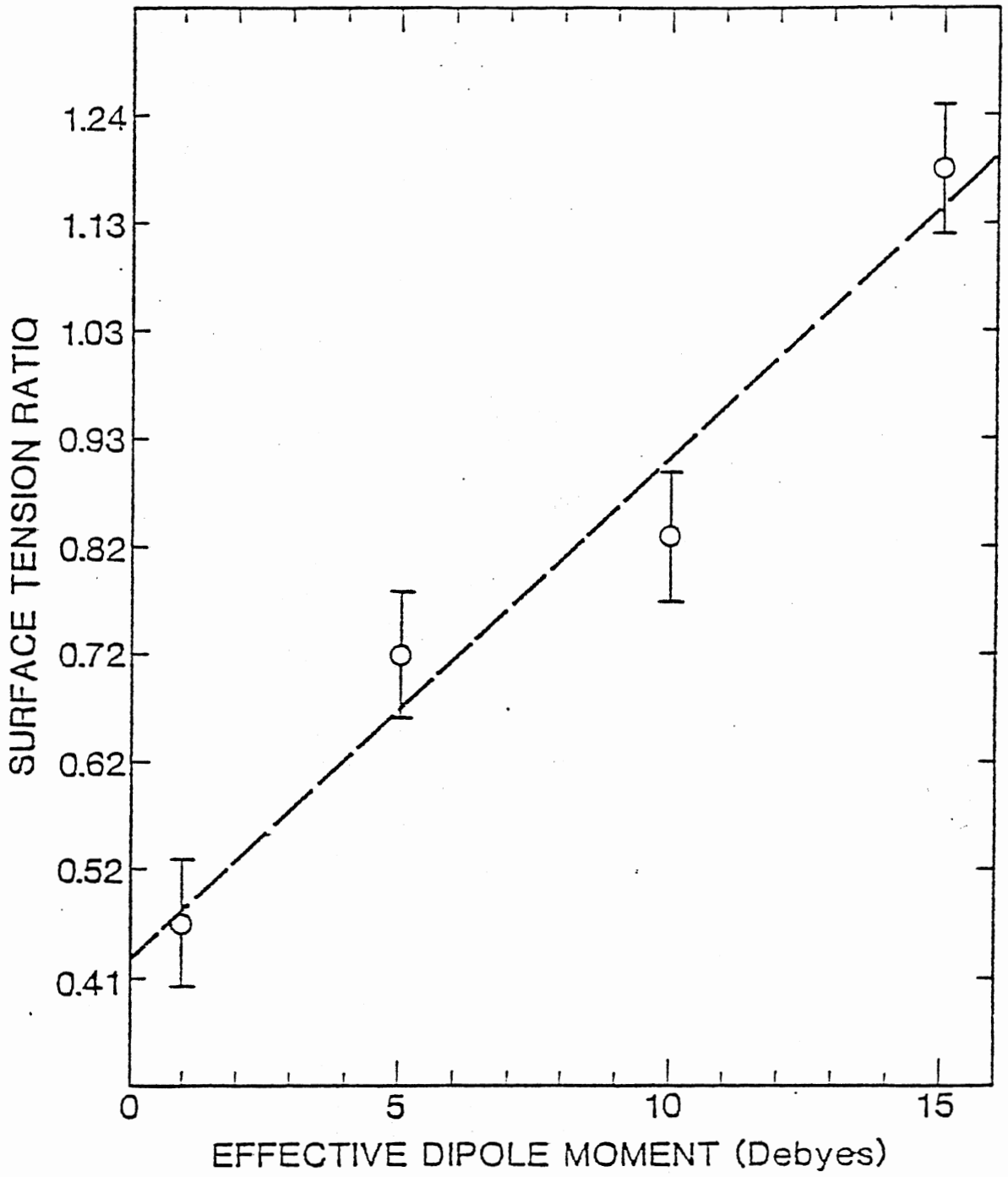

Figure 11. A Plot of the Ratio of the Calculated Film Surface Tension to the Calculated Water Surface Tension Vs. Effective Dipole Moment of the Head Group. Error Bars are ± 0.06 (± 6 Dynes/cm)

CHAPTER VI

DISCUSSION AND CONCLUSION

In Chapter II, we have demonstrated that the half-umbrella sampling is superior to the Metropolis sampling. By comparing Figure 3b and 3c, we see that, if an optimum weighting function is used, the Torrie-Valleau sampling should be more efficient than the half-umbrella sampling. However, to search for an optimum weighting function is a tedious task and usually requires a considerable number of steps, and this tends to negate the advantage given by using this approach.

In the surface tension calculation, the half-umbrella sampling is applied to calculate the major contribution, $F_c - F_b$. We have shown that the number of Monte Carlo steps required for accurately evaluating the free energy difference depends on its "important range". In Table I, we note that the important range of a given free energy difference is <u>not</u> related to its magnitude, but seems to depend on the complexity of the interaction potentials. For the last stage, from 3.2Å to 9.8Å, ΔU_j^* actually involves calculations of ST2 potentials in which all the water-water distances are beyond 3.2Å. Thus, ΔU_j^* is essentially dominated by dipole-dipole interactions. The important range in ΔU^* of this stage is only about 10, which is smaller than that of the other stages with even smaller separation. In Chapter II, we also found that the important range for the Lennard-Jones particles is small (about 8). This result is reasonable because the free energy is essentially the

logarithm of the "partition function" (summation over all possible configurations). When the interaction potentials have more variables, more distinct configurations are possible and, thus, more steps are required for an accurate Monte Carlo sampling.

If the important range is not covered by the Monte Carlo walk, the error can be very large. For example, from $d_j = 0$ to $d_{j+1} = 0.5\text{Å}$, we expect from Table I that $\ell n\langle \exp(\Delta U_j^*)\rangle_j = -(0.1 + 0.7 + 5.3) \pm 1.3 = -6.1 \pm 1.3$. However, if we do it in a single stage instead of several steps, we get $\ell n\langle \exp(\Delta U_j^*)\rangle \approx 18$ after 1.5×10^5 steps with the one-half umbrella sampling algorithm. The latter result is in error because the important range of ΔU^* is far from being covered by 1.5×10^5 steps when the separation is large. In TAble I, the stage from $d_j = 2.5\text{Å}$ to $d_{j+1} = 3.2\text{Å}$ has the largest contribution. As a check, we divide it into two stages, $2.5\text{Å} \rightarrow 2.85\text{Å}$ and $2.85\text{Å} \rightarrow 3.2\text{Å}$. The sum of their free energy difference is consistent with the free energy difference of the stage from 2.5Å to 3.2Å.

The relaxation effect, is obtained by calculating N_{out}, the number of molecules which move out of the two surfaces after the two hard walls are released. For the pure water, the model system actually contains vacuum/water interfaces, instead of air/water interfaces. One may argue that the liquid water in vacuum should evaporate indefinitely so that $\langle N_{out}\rangle$ would be very large. In our Monte Carlo simulation, $\langle N_{out}\rangle$ was only 5.6 ± 0.4 after 10^5 steps, and this value did not seem to increase (within the error of the computation) for the subsequent 10^5 steps. Thus, the expected increase of $\langle N_{out}\rangle$ in vacuum/water interfaces should be very small after 10^5 steps. This slight increase is likely to be canceled by the air pressure when the real system, the

air/water interfaces, is considered. In our results the term, $F_d - F_c$ contributes only about 3% of the total surface tension, which is small compared with 13% obtained by Miyazaki et al. (15) for argon. This is expected because the surface tension of argon was evaluated at critical temperature (actually the triple point) while in the present calculation, the surface tension of water is evaluated at room temperature ($25^{o}C$).

The calculated surface tension of water, 97 dynes/cm, is considerably larger than the experimental value of 72 dynes/cm. This overestimation is most likely due to the following reasons: (1) the ST2 potential does not accurately represent the interaction potentials of water molecules for the calculations presented here, (2) the model system is too small so that the effects of boundary conditions are significant and the center of the slab is still affected by the surfaces. In either case there is no simple remedy available. However, this result can serve as a basis for comparing pure water interfaces with lipid/water interfaces, because when differences are considered one expects much of the error due to the above two reasons to cancel.

Usually the surface tension of the lipid/water interface is not obtained by a direct measurement, but from the surface pressure which is defined by

$$\pi \equiv \gamma_o - \gamma_{LW} \tag{51}$$

where γ_o is the surface tension of the air/water interface. Substituting Equation (50) into Equation (51), we have

$$\pi = \gamma_o - \gamma_{hw} - \gamma_{ca} + \pi_{cc} \tag{52}$$

For dipalmitoyl phosphatidylcholine (DPPC) at 25°C and 50Å^2/lipid, the surface pressure is about 18 dynes/cm (30). Theoretical studies suggest that the chain pressure of DPPC at 25°C is ~10 dynes/cm and the chain/air surface tension is roughly about 20 dynes (31). Equation (52) thus yields γ_{hw} ~ 44 dynes/cm. This measn the ratio of γ_{hw}/γ_o = 44/72 = 0.61. From Figure 11, we then estimate that the effective dipole moment is ~ 4 debyes.

In conclusion, we have developed an efficient method for the calculation of the surface tension of air/water and lipid/water interfaces. Although at this time the calculated values are not in good agreement with experiments (possibly due to the ST2 potential or the small size of the model system), the relative magnitude of the calculated values should be accurate. In this study, these values have been used to estimate the effective dipole moment of the head group at surface. In the near future, one may apply the method to study the effects of the head group size or the head group density on the surface pressure. The method can also be applied to most of the other interfacial systems.

REFERENCES

1. Hair, H. L., The Chemistry of Biosurfaces, Vol. 1,2 (Marcel Dekker, New York, 1971).

2. Davies, J. T. and E. K. Ridecl, Interfacial Phenomena (Academic Press, New York, 1963).

3. Rice, O. K., Statistical Mechanics: Thermodynamics and Kinetics (Freeman Co., San Francisco, 1967).

4. Brown, R. C., Contemp. Phys. 15, 301 (1974).

5. Kirkwood, J. G. and F. P. Buff, J. Chem. Phys. 17 338 (1949).

6. Pathria, R. K., Statistical Mechanics (Pergamon, Oxford, 1977).

7. Bennett, C. H., J. Computa. Phys. 22, 245 (1976).

8. Stillinger, F. H. and A. Rahmen, J. Chem. Phys. 60 1545 (1974).

9. Matsuoka, O., E. Clementi and M. Yoshimina, J. Chem. Phys. 64, 1351 (1976).

10. Ladd, A. J. C., Mol. Phys. 33, 1039 (1977).

11. Mezei, M., S. Swaminathan and D. L. Beveridge, J. Chem. Phys. 71, 3366 (1979).

12. Dorsey, N. E., Properties of Ordinary Water-Substance (Reinhold, New York, 1940).

13. Lie, G. C., E. Clementi and M. Yoshimine, J. Chem. Phys. 64, 2314 (1976).

14. Lee, J. K., J. A. Barker and G. M. Pound, J. Chem. Phys. 60, 1976 (1974).

15. Miyazaki, J., J. A. Barker, and G. M. Pound, J. Chem. Phys. 64, 3364 (1976).

16. Rao, M. and D. LeVesque, J. Chem. Phys. 65, 3233 (1976).

17. Metropolis, N., A. W. Rosenbluth, M. N. Rosenbluth, A. H. Teller, and E. Teller, J. Chem. Phys. 21, 1087 (1953).

18. Scott, H. L., Biochim. Biophys. Acta, 469, 264 (1977).

19. Torrie, G. M. and J. P. Valleau, Chem. Phys. Lett. 29, 578 (1974).

20. Torrie, G. M. and J. P. Valleau, J. Computa. Phys. 23, 187 (1977).

21. Valleau, J. P. and S. G. Whittington, in Modern Theoretical Chemistry, ed. B. J. Berne, Vol. 5 (Plenum, New York, 1977).

22. Fröhlich, H., Theory of Dielectrics (Clarendon, Oxford, 1958).

23. Arfken, G., Mathematical Methods for Physicists (Academic Press, New York, 1970).

24. Eisenberg, D. and W. Kauzmann, The Structure and Properties of Water (Oxford Press, London, 1969).

25. Weast, R. C., Handbook of Chemistry and Physics (CRC Press, Florida, 1979), 60th ed., P. F-45.

26. Seelig, J., H. U. Gally and R. Wohlgemuth, Biochim Biophys. Acta, 467, 109 (1977).

27. Scott, H. L., Biochim. Biophys. Acta, 406, 329 (1975).

28. Scott, H. L. and W. H. Cheng, J. Coll. Int. Sci. 62, 125 (1977).

29. Nagle, J. F., Ann. Rev. Phys. Chem., In Press (1980).

30. Albrecht, D., H. Gruler and E. Sackmann, J. de Physique 39, 301 (1978).

31. Nagle, J. F., J. Memb. Biol. 27, 233 (1976).

32. Hammersley, J. M. and D. C. Handscomb, Monte Carlo Methods (Methuen, London, 1964).

33. Chung, K. L., Markov Chains With Stationary Transition Probabilities (Springer, Berlin, 1960).

APPENDIX A

DERIVATION OF KIRKWOOD-BUFF FORMULA

Consider that an assembly of molecules is confined in a rectangular container with edges extending from the origin to a, b, c in the x, y, z directions, respectively (Figure 1). Let m be the mass of each molecule, x_i, y_i, z_i be the Cartesian coordinates of the ith molecule and f_{xi}, f_{yi}, f_{zi} be the components of the force exerted upon it. Then

$$x_i f_{xi} = x_i \frac{d(m\dot{x}_i)}{dt} = \frac{d(x_i m\dot{x}_i)}{dt} - m\dot{x}_i^2 \qquad (A.1)$$

In a stationary system the sum of the velocities $\dot{x}_i$ over the molecules at or near some specific value of x_i must be zero (otherwise there would be a net flux into or out of the region around the specific x_i. Thus

$$\Sigma\, d(x_i m\dot{x}_i)/dt = \frac{d}{dt} \Sigma\, x_i m\dot{x}_i = 0 \qquad (A.2)$$

and therefore

$$\Sigma\, x_i\, f_{xi} = -\Sigma\, m\dot{x}_i^2 = -NkT \qquad (A.3)$$

where N is the number of molecules in the container. The forces in this system are of two kinds--intermolecular forces and forces between the molecules of the assembly and the walls. If the force between any pair of molecules, i and j, is a function of the distance r_{ij}, and the force on any given molecule can be obtained by adding vectorically the forces due to all its neighbors, then

$$f_{xi} = \sum_j \frac{-u'(r_{ij})(x_i - x_j)}{r_{ij}} \qquad (A.4)$$

where $u'(r_{ij})$ is the derivative of the intermolecular potential $u(r_{ij})$. Furthermore,

$$\sum_i{}' x_i f_{xi} = \sum_i \sum_j \frac{-x_i\, u'(r_{ij})(x_i - x_j)}{r_{ij}} \tag{A.5}$$

The prime on the summation sign means that the effect of the wall is not included. We may interchange i and j on the right-hand side, since they both range over all molecules. Then Equation (A.5) becomes

$$\sum_i{}' x_i f_{xi} = \sum_i \sum_j \frac{-x_j\, u'(r_{ij})(x_j - x_i)}{r_{ij}} \tag{A.6}$$

and adding the two expressions

$$\sum_i{}' x_i f_{xi} = \frac{1}{2} \sum_i \sum_j \frac{-(x_i - x_j)^2\, u'(r_{ij})}{r_{ij}}$$

$$= -\sum_{i>j} \frac{x_{ij}^2\, u'(r_{ij})}{r_{ij}} \tag{A.7}$$

Let F_x be the force exerted by one of the yz faces of the container if there were no interfaces between a liquid and a gas, then $F_x = Pbc$. As explained in the Introduction, the presence of interface will reduce the force by an amount ΔF_x. Thus, from Equations (A.3) and (A.7),

$$-(F_x + \Delta F_x)a + \sum_{i>j} \frac{-x_{ij}^2\, u'(r_{ij})}{r_{ij}} = -NkT \tag{A.8}$$

Similarly, for the z direction, we have

$$- cF_z = \sum_{i>j} \frac{- z_{ij}^2 \, u'(r_{ij})}{r_{ij}} = - NkT \qquad (A.9)$$

Since $aF_x = Pabc = cF_z$, we see by subtracting Equation (A.9) from Equation (A.8)

$$- a\Delta F_x - \sum_{i>j} \frac{(x_{ij}^2 - z_{ij}^2) \, u'(r_{ij})}{r_{ij}} = 0 \qquad (A.10)$$

According to Equation (1) of the text and assuming that the distribution of the configurations is "canonical" (i.e., the probability that a system is found to be in one of the configurations characterized by the energy U_s is proportional to $\exp(-U_s/kT)$), Equation (A.10) leads to the Kirkwood-Buff formula, Equation (2) of the text.

APPENDIX B

THE METROPOLIS MONTE CARLO WALK AS A MARKOV CHAIN

The Metropolis Monte Carlo walk is a realization of a "Markov chain" which is defined as follows: Let the points in a configuration space Γ be numbered 1,2,3,..... and consider a random walker on these points. We are concerned with the conditional probability that the walker is at point k_j at step (t+1) given that it was at point k_o at step 0, k_1 at step 1, ..., and k_i at step t. We write this conditional probability as

$$\Pr\{k_j,t+1|k_i,t;\ .....;\ k_1,1;\ k_o,0\}$$

If the memory of the process extends back only one step, so that

$$\Pr\{k_j,t+1|k_i,t;\ ....\ k_1,1;\ k_o,0\} = \Pr\{k_j,t+1|k_i,t\} \qquad (B.1)$$

then the process is called a Markov chain. For the Metropolis Monte Carlo walk, the transition probability is independent of t. We write

$$\Pr\{k_j,t+1|k_i,t\} = P_{ij} \qquad (B.2)$$

Let P^*_{ij} be the transition probability of a Metropolis trial move between two configurations, i and j (not including procedure (iv)). It satisfies

$$p^*_{ij} \geq 0; \quad \sum_j p^*_{ij} = 1, \quad p^*_{ij} = p^*_{ji} \qquad (B.3)$$

With the acceptance or rejection procedure, (iv), the transition probability becomes

$$\begin{aligned} p_{ij} &= p^*_{ij} && \pi_j \geq \pi_i \quad j \neq i \\ &\quad p^*_{ij}\,\pi_j/\pi_i && \pi_j < \pi_i \quad j \neq i \end{aligned} \qquad (B.4)$$

$$p_{ii} = 1 - \sum_{j \neq i} p_{ij}$$

where in the Metropolis sampling,

$$\pi_s = \frac{e^{-U_s/kT}}{\sum_{s \in \Gamma} e^{-U_s/kT}} \tag{B.5}$$

It is easy to show (32) that Equation (B.4) satisfies the following conditions for any distribution π_s,

$$p_{ij} \geq 0, \quad \sum_j p_{ij} = 1, \quad \sum_i \pi_i p_{ij} = \pi_j \tag{B.6}$$

A Markov chain satisfying Equation (B.6) is called "irreducible". For an irreducible Markov chain, the average of a quantity g is given by

$$\frac{1}{n} \sum_{t=1}^{n} g_t = \sum_{s \in \Gamma} g_s \pi_s + O(n^{-1/2}) \tag{B.7}$$

(33). The second term, $O(n^{-1/2})$, becomes negligible as n goes to infinity. If the distribution π_s is given by Equation (B.5), Equation (B.7) leads to Equation (17) of the text. In the umbrella-sampling method (see Chapter II), the distribution is chosen to be

$$\pi_s = \frac{W_s e^{-U_s/kT}}{\sum_{s \in \Gamma} W_s e^{-U_s/kT}} \tag{B.8}$$

where W_s is an arbitrary function of configurations.

The Metropolis transition probability, Equation (B.4), is not a unique choice to satisfy the irreducible conditions of a Markov chain. An alternative, referred to as Barker sampling (21), is given below

$$p_{ij} = p^{*}_{ij}\, \pi_j/(\pi_i+\pi_j)$$

$$p_{ii} = 1 - \sum_{j\neq i} p_{ij} \qquad \text{(B.9)}$$

However, it has been shown (21) that the Metropolis sampling, in most cases, converges faster than the Barker sampling.

APPENDIX C

COMPUTER PROGRAM FOR THE CALCULATION OF THE FREE ENERGY CHANGE IN SEPARATING SLAB SHAPED LIQUIDS

```
      COMMON /A/L,K,X(256),Y(256),Z(256)
      COMMON /C/AX(4,256),AY(4,256),AZ(4,256)
      COMMON /E/THET(256),PHI(256),CTT(256),STT(256)
      COMMON /IMP/DD
      COMMON /L/LG
      COMMON /M/XM(256),YM(256),ZM(256)
      COMMON /MONU/DV
      COMMON /S/SIZEX,SIZEY,RC
      DIMENSION AXL(4),AYL(4),AZL(4)
      DIMENSION BX(4,256),BY(4,256),BZ(4)
      DIMENSION BXS(4),BYS(4),SWF(256)
      DIMENSION CX(4),CY(4)
      DIMENSION E(255,128),EL(256)
      NQUIT=150
      NNN=5
       NAV=256
       N=256
      PI=3.141593
       RC=9.8
C     *** RC IS THE CUTOFF DISTANCE
      RC2=RC**2
      BKT=0.592
C     *** BOLTZMANN CONSTANT TIMES TEMPERATURE AT 298 K,
C         UNIT KCAL/MOLE
C
       DMIN=-50.
       SIZE=19.72
       SIZEX=SIZE
       SIZEY=SIZE
       SIZEZ=SIZE
       DELA=0.13
       DELR=0.13
C     *** MAXIMUM ALLOWED DISPLACEMENT
C
       SEPA0=0.
       SEPA1=0.15
C     *** SLAB SEPARATIONS IN SYSTEMS 0 AND 1
C
        ZP0=SIZEZ+SEPA0
        ZP1=SIZEZ+SEPA1
9      FORMAT(/,5X,I7)
1550   FORMAT(//,5X,I7,3E20.7)
1560   FORMAT(10X,'AV.EXP(-DU)/W=',E18.7,10X,'AV.1/W=',E18.7)
1570   FORMAT(20X,'RATIO=',E20.7)
6230   FORMAT(2X,8(I4,E10.3))
6240   FORMAT(2X,8(I6,F8.0))
      OM=0.57735
      CX(1)=0.8*OM
      CY(1)=0.8*OM
      CX(2)=OM
      CY(2)=-OM
```

```
      CX(3)=-0.8*OM
      CY(3)=-0.8*OM
      CX(4)=-OM
      CY(4)=OM
      BZ(1)=-0.8*OM
      BZ(2)=OM
      BZ(3)=-0.8*OM
      BZ(4)=OM
       DO 55 L=1,N
      ROT=PI*RANF(0)
      CA=COS(ROT)
      SA=SIN(ROT)
      DO 50 M=1,4
      BX(M,L)=SA*CY(M)+CA*CX(M)
      BY(M,L)=CA*CY(M)-SA*CX(M)
50    CONTINUE
      THET(L)=PI*RANF(0)
      PHI(L)=2.*PI*RANF(0)
      CTT(L)=COS(THET(L))
      STT(L)=SIN(THET(L))
      CP=COS(PHI(L))
      SP=SIN(PHI(L))
      DO 53 M=1,4
      AX(M,L)=CTT(L)*CP*BX(M,L)-SP*BY(M,L)+STT(L)*CP*BZ(M)
      AY(M,L)=CTT(L)*SP*BX(M,L)+CP*BY(M,L)+STT(L)*SP*BZ(M)
      AZ(M,L)=-STT(L)*BX(M,L)+CTT(L)*BZ(M)
53    CONTINUE
55    CONTINUE
C     *** AX(M,L),AY(M,L),AZ(M,L) ARE THE SPACE COORDINATES
C       OF THE M-TH (M=1,4) CHARGE OF L-TH MOLECULE
C
      X(1)=SIZEX/2.
      Y(1)=SIZEY/2.
      Z(1)=SIZEZ/2.
      L=1
205   L=L+1
208   XR=RANF(0)
      ZR=RANF(0)
      YR=RANF(0)
      X(L)=SIZEX*XR
      Y(L)=SIZEY*YR
      Z(L)=SIZEZ*ZR
      LM1=L-1
       DO 209 K=1,LM1
        CALL DIST(X(L),Y(L),Z(L),ZP0,RKL)
       IF (RKL .LT. 5.) GO TO 208
209   CONTINUE
      IF (L .LT. N) GO TO 205
C     *** END OF PICKING UP AN INITIAL CONFIGURATION
C
      XM(1)=(AX(2,1)+AX(4,1))/2.
      YM(1)=(AY(2,1)+AY(4,1))/2.
      ZM(1)=(AZ(2,1)+AZ(4,1))/2.
```

```
        DO 230 L=2,N
      XM(L)=(AX(2,L)+AX(4,L))/2.
      YM(L)=(AY(2,L)+AY(4,L))/2.
      ZM(L)=(AZ(2,L)+AZ(4,L))/2.
C     (XM,YM,ZM) REPRESENTS THE VECTOR OF THE DIPOLAR AXIS
      DO 215 M=1,4
      AXL(M)=AX(M,L)
      AYL(M)=AY(M,L)
      AZL(M)=AZ(M,L)
215   CONTINUE
      LM1=L-1
      DO 220 K=1,LM1
       CALL DIST(X(L),Y(L),Z(L),ZP0,RL)
      IF (RL .GT. RC2) GO TO 220
      CALL ENERGY(RL,AXL,AYL,AZL,XM(L),YM(L),ZM(L),U)
      CALL INDEX(KI,LI)
      E(KI,LI)=U
        UINS=UINS+U
       IF (LG .EQ. 1) GO TO 233
C     *** C.F. SUBROUTINE DIST
       UINS1=UINS1+U
       GO TO 220
233    CALL DIST(X(L),Y(L),Z(L),ZP1,RL)
       IF (RL .GT. RC2) GO TO 220
      CALL ENERGY(RL,AXL,AYL,AZL,XM(L),YM(L),ZM(L),U)
       UINS1=UINS1+U
220    CONTINUE
230   CONTINUE
C
C     *** UINS AND UINS1 ARE THE  INSTANTANEOUS POTENTIAL
C       ENERGY OF SYSTEMS 0 AND 1,RESPECTIVELY
C
        DUINS=(UINS1-UINS)/BKT
          I=DUINS-DMIN

       WRITE (6,9) I
       FOW=EXP(-DUINS/2.)
      KOUNT=0
10    DO 1900 KPASS=1,NQUIT
       DO 1600 KSTEP=1,NNN
       DO 1400 L=1,NAV
        KKK=KKK+1
      XS=X(L)
      YS=Y(L)
      ZS=Z(L)
      THETS=THET(L)
      PHIS=PHI(L)
      CTTS=CTT(L)
      STTS=STT(L)
       DO 580 M=1,4
      BXS(M)=BX(M,L)
      BYS(M)=BY(M,L)
580   CONTINUE
```

```
      DO 255 M=1,4
      AXL(M)=AX(M,L)
      AYL(M)=AY(M,L)
      AZL(M)=AZ(M,L)
255   CONTINUE
C     *** SAVE THE COORDINATES OF THE OLD CONFIGURATION
C
        ULS=0.
        ULTS=0.
        UL1S=0.
        DO 258 K=1,N
        IF (K .EQ. L) GO TO 258
        CALL DIST(XS,YS,ZS,ZP0,RL)
        IF (RL .GT. RC2) GO TO 258
        CALL INDEX(KI,LI)
        ULS=ULS+E(KI,LI)
        IF (LG .NE. 1) GO TO 258
C     *** C.F. SUBROUTINE DIST
C
       ULTS=ULTS+E(KI,LI)
       CALL DIST(XS,YS,ZS,ZP1,RL)
       IF (RL .GT. RC2) GO TO 258
      CALL ENERGY(RL,AXL,AYL,AZL,XM(L),YM(L),ZM(L),U)
       UL1S=UL1S+U
258   CONTINUE
C     *** ULS IS THE INTERACTION ENERGY OF THE L-TH MOLECULE
C     WITH ITS SURROUNDING MOLECULES IN THE OLD CONFIGURA-
C     TION OF SYSTEM 0
C     *** ULTS IS THE PORTION OF THE INTERACTION ENERGY IN
C     SYSTEM 0, WHICH MAY BE DIFFERENT FROM THAT IN SYSTEM 1
C     *** UL1S IS THE PORTION OF THE INTERACTION ENERGY IN
C     SYSTEM 1, WHICH MAY BE DIFFERENT FROM THAT IN SYSTEM 0
C
450   TZ=RANF(0)
       TZM=DELR*(1.-TZ*2.)
      Z(L)=ZS+TZM
      IF (Z(L) .LT. 0.) GO TO 1150
      IF (Z(L) .GT. SIZEZ) GO TO 1150
260   TX=RANF(0)
       TXM=DELR*(1.-TX*2.)
      X(L)=XS+TXM
      IF (X(L) .LE. SIZEX) GO TO 300
      X(L)=X(L)-SIZEX
      GO TO 350
300   IF (X(L) .GT. 0.) GO TO 350
      X(L)=X(L)+SIZEX
350   TY=RANF(0)
       TYM=DELR*(1.-TY*2.)
      Y(L)=YS+TYM
      IF (Y(L) .LE. SIZEY) GO TO 400
      Y(L)=Y(L)-SIZEY
       GO TO 575
400    IF (Y(L) .GT. 0.) GO TO 575
      Y(L)=Y(L)+SIZEY
```

```
575     RO=RANF(0)
        ROT=DELA*(1.-RO*2.)
        CA=COS(ROT)
        SA=SIN(ROT)
        DO 600 M=1,2
         BX(M,L)=SA*BYS(M)+CA*BXS(M)
         BY(M,L)=CA*BYS(M)-SA*BXS(M)
600     CONTINUE
        BX(3,L)=-BX(1,L)
        BY(3,L)=-BY(1,L)
        BX(4,L)=-BX(2,L)
        BY(4,L)=-BY(2,L)
700     RT=RANF(0)
        RTM=DELA*(1.-RT*2.)
        THET(L)=THETS+RTM
        IF (THET(L) .GE. PI .OR. THET(L) .LT. 0.) GO TO 700
        CTT(L)=COS(THET(L))
        STT(L)=SIN(THET(L))
750     RP=RANF(0)
        RPM=DELA*(1.-RP*2.)
        PHI(L)=PHIS+RPM
790     CP=COS(PHI(L))
        SP=SIN(PHI(L))
        CTCP=CTT(L)*CP
        STCP=STT(L)*CP
        CTSP=CTT(L)*SP
        STSP=STT(L)*SP
        DO 920 M=1,4
        AXL(M)=CTCP*BX(M,L)-SP*BY(M,L)+STCP*BZ(M)
        AYL(M)=CTSP*BX(M,L)+CP*BY(M,L)+STSP*BZ(M)
        AZL(M)=-STT(L)*BX(M,L)+CTT(L)*BZ(M)
920     CONTINUE
C           **************************
         UL=0.
         ULT=0.
         UL1=0.
        XML=(AXL(2)+AXL(4))/2.
        YML=(AYL(2)+AYL(4))/2.
        ZML=(AZL(2)+AZL(4))/2.
          DO 1000 K=1,N
        IF (K .EQ. L) GO TO 1000
        CALL INDEX(KI,LI)
        CALL DIST(X(L),Y(L),Z(L),ZP0,RL)
        IF (RL .GT. RC2) GO TO 975
        CALL ENERGY(RL,AXL,AYL,AZL,XML,YML,ZML,U)
        EL(K)=U
        UL=UL+U
         IF (LG .NE. 1) GO TO 1000
         ULT=ULT+U
         CALL DIST(X(L),Y(L),Z(L),ZP1,RL)
         IF (RL .GT. RC2) GO TO 1000
        CALL ENERGY(RL,AXL,AYL,AZL,XML,YML,ZML,U)
         UL1=UL1+U
        GO TO 1000
```

```
975    EL(K)=E(KI,LI)
1000   CONTINUE
        UMU=UL1-ULT
        UMUS=UL1S-ULTS
         DD=(UMU-UMUS)/BKT
1100   CALL CHECK (UL,ULS,NY)
       IF (NY .EQ. 1) GO TO 1300
C      *** IF NY=1, THE TRANSITION IS ACCEPTED
C          OTHERWISE, IT IS REJECTED
C
1150    X(L)=XS
       Y(L)=YS
       Z(L)=ZS
       THET(L)=THETS
       PHI(L)=PHIS
       CTT(L)=CTTS
       STT(L)=STTS
       DO 1200 M=1,4
       BX(M,L)=BXS(M)
       BY(M,L)=BYS(M)
1200   CONTINUE
        GO TO 1390
C
1300   UINS=UINS+DV
       KOUNT=KOUNT+1
1305   XM(L)=XML
       YM(L)=YML
       ZM(L)=ZML
       DO 1310 M=1,4
       AX(M,L)=AXL(M)
       AY(M,L)=AYL(M)
       AZ(M,L)=AZL(M)
1310   CONTINUE
         DO 1350 K=1,N
       IF (K .EQ. L) GO TO 1350
       CALL INDEX(KI,LI)
       E(KI,LI)=EL(K)
1350   CONTINUE
        DUINS=DUINS+DD
        FOW=EXP(-DUINS/2.)
1390    WFT=WFT+EXP(DUINS/2.)
         FOWT=FOWT+FOW
           I=DUINS-DMIN

         SWF(I)=SWF(I)+1.
1400   CONTINUE
1600   CONTINUE
        WRITE (6,1550) KKK,UINS,FOW,WFS
        FAV=FOWT/KKK
        WFAV=WFT/KKK
        WRITE (6,1560) FAV,WFAV
        RAT=FAV/WFAV
        WRITE (6,1570) RAT
        WRITE (6,6235)
```

```
6235   FORMAT(/,5X,'PROBABILITY DISTRIBUTION')
       DO 1750 M=1,16
       NBEG=(M-1)*8+1
       NEND=NBEG+7
       WRITE (6,6240) ((J,SWF(J)),J=NBEG,NEND)
1750   CONTINUE
1900  CONTINUE
       WRITE (6,1550) KKK,USUM,FOWT,WFT
       WRITE (6,9) KOUNT
       WRITE (56) X,Y,Z,BX,BY,THET,PHI,SWF
C      *** STORE THE DATA AT THIS STEP IN DISK
C
      STOP
      END
C
C
C
      SUBROUTINE INDEX(KI,LI)
      COMMON /A/L,K
C     STORING THE POTENTIAL ENERGY OF ALL PAIRS, E(K,L), WILL
C     SAVE COMPUTATION TIME SUBSTANTIALLY.  HOWEVER, THE
C     MEMMORY CAPACITY OF IBM 370/158 IS NOT SUFFICIENT TO
C     STORE E(256,256).  SINCE E(K,L)=E(L,K),WE ACTUALLY
C     NEED ONLY 255X128 ADDRESSES.  THIS SUBROUTINE IS TO
C     STORE E(1,2) IN E(255,2),(1,3) IN (255,3),(2,3) IN
C     (254,3),........, (127,128) IN (129,128); (1,129) IN
C     (1,128), (2,129) IN (2,128),..,(255,256) IN (255,1)
      IF (K .LT. L) GO TO 940
      LI=K
      KI=L
      GO TO 950
940   LI=L
      KI=K
950   IF (LI .GT. 128) GO TO 960
      KI=256-KI
      GO TO 970
960   LI=257-LI
970   RETURN
      END
C
C
C
      SUBROUTINE ENERGY(RKL,AXL,AYL,AZL,XML,YML,ZML,U)
      COMMON /A/L,K
      COMMON /B/D(3)
      COMMON /C/AX(4,256),AY(4,256),AZ(4,256)
      COMMON /E/THET(256),PHI(256),CTT(256),STT(256)
      COMMON /M/XM(256),YM(256),ZM(256)
      DIMENSION AXL(4),AYL(4),AZL(4)
C        UNIT KCAL/MOLE
C
       IF (RKL .GT. 50.) GO TO 100
      AB=(9.61/RKL)**3
```

```
      VLJ=0.303*(AB*AB-AB)
      VEL=0.
      SGNJ=1.
      DO 70 J=1,4
      A1=D(1)-AX(J,K)
      A2=D(2)-AY(J,K)
      A3=D(3)-AZ(J,K)
      SGN=SGNJ
      DO 60 I=1,4
      DR=SQRT((A1+AXL(I))**2+(A2+AYL(I))**2+(A3+AZL(I))**2)
      VEL=VEL+18.4366*SGN/DR
60    SGN=-SGN
70    SGNJ=-SGNJ
      IF (RKL .GE.  9.78876) GO TO 90
      R=SQRT(RKL)
      U=VLJ+VEL*(R-2.0160)**2*(7.3701-2.*R)/1.2381
      GO TO 200
90    U=VLJ+VEL
      GO TO 200
C
C     *** THE FOLLOWING IS DIPOLE-DIPOLE APPROXIMATION
100   R=SQRT(RKL)
      DIPL=XML*D(1)+YML*D(2)+ZML*D(3)
      DIPK=XM(K)*D(1)+YM(K)*D(2)+ZM(K)*D(3)
      PROJ=CTT(L)*CTT(K)+STT(L)*STT(K)*COS(PHI(L)-PHI(K))
      R3=R*RKL
       UAA=(PROJ-9.*DIPL*DIPK/RKL)/R3
150    U=79.666*UAA
200   RETURN
      END
C
C
C
        SUBROUTINE DIST(XL,YL,ZL,SIZEZ,RL)
      COMMON /A/L,K,XYZ(256,3)
      COMMON /B/D(3)
      COMMON /L/LG
      COMMON /S/SIZE(2),RC
C
C     THE PROGRAM IS TO CALCULATE THE DISTANCE BETWEEN K-TH
C       AND L-TH MOLECULES WITH PERIODIC BOUNDARY CONDITIONS
C
        LG=0
      D(1)=XL-XYZ(K,1)
      D(2)=YL-XYZ(K,2)
      D(3)=ZL-XYZ(K,3)
        DO 50 I=1,2
      IF (D(I) .LE. RC) GO TO 20
      D(I)=D(I)-SIZE(I)
      IF (ABS(D(I)) .GT. RC) GO TO 60
      GO TO 50
20    IF (D(I) .LT. -RC) GO TO 30
      GO TO 50
```

```
30    D(I)=D(I)+SIZE(I)
      IF (ABS(D(I)) .GT. RC) GO TO 60
50    CONTINUE
        IF (D(3) .LE. RC) GO TO 51
        D(3)=D(3)-SIZEZ
        IF (ABS(D(3)) .GT. RC) GO TO 60
        LG=1
        GO TO 55
51      IF (D(3) .GT. -RC) GO TO 55
        D(3)=D(3)+SIZEZ
        IF (ABS(D(3)) .GT. RC) GO TO 60
        LG=1
C     *** IF LG=1, THE INTERACTION ENERGIES BETWEEN L-TH
C       AND K-TH MOLECULES ARE DIFFERENT FOR THE TWO SYSTEMS
C       0 AND 1;  IF LG=0, THEY ARE THE SAME
C
55    RL=D(1)**2+D(2)**2+D(3)**2
      GO TO 70
60    RL=RC**2+1.0
C     *** RL HERE IS GREATER THAN THE CUTOFF DISTANCE.  THE
C       INTERACTION WILL BE NEGLECTED,  SEE MAIN PROGRAM
C
70    RETURN
      END



       SUBROUTINE CHECK(U,US,NY)
      COMMON /IMP/DD
      COMMON /MONU/DE
      BKT=0.592
C
C        TEMPERATURE=298 K
C        UNIT KCAL/MOLE
C        ***********
      DE=U-US
      DU=DE/BKT
       ARG=DU+DD/2.
C     *** IF ARG=DU, THE HALF-UMBRELLA SAMPLING REDUCES
C       TO THE METROPOLIS MONTE CARLO SAMPLING
        IF (ARG .LT. 0.) GO TO 200
        IF (ARG .GT. 15.) GO TO 100
C     *** TO AVOID UNDERFLOW IN THE NEXT STATEMENT
        DP=EXP(-ARG)
      RAN=RANF(0)
      IF (DP .GT. RAN) GO TO 200
100   NY=0
      GO TO 300
200   NY=1
300   RETURN
      END
```

```
//GO.FT56F001 DD DSN=OSU.ACT13029.SCOB,DISP=(NEW,KEEP),
//     UNIT=3350,VOL=SER=DASD40,SPACE=(1032,15),
//     DCB=(BLKSIZE=3120,LRECL=1028,RECFM=VBS)
C
C
C      *** THE FUNCTION RANF(0) GENERATES RANDOM NUMBERS
C      UNIFORMLY DISTRIBUTED BETWEEN 0 AND 1.  ITS PROGRAM
C      IS WRITTEN BY DR. J.P. CHANDLER OF THE OSU COMPUTER
C      SCIENCE DEPARTMENT AND IS OMITTED HERE.  THE SUBROU-
C      TINE ENERGY IS ALSO IMPROVED BY DR. CHANDLER.
```

APPENDIX D

ORIENTATION OF THE WATER MOLECULES NEAR SURFACE

The structure of water is important in many biological and chemical systems. For this reason, it is interesting to obtain some information about the orientation of the water molecules near surface. As described in Chapter IV, the orientation of water molecules can be specified by three Euler angles θ, ψ, and α, where θ and ψ denote the spherical polar and azimuthal angles of the dipolar axis (pointing from the oxygen to the middle point of the two hydrogens), α represents the rotational angle of the molecule about the dipolar axis. If the normal to the water surface is taken to be the z-axis, then $\theta = 0^{\circ}$ and $\theta = 90^{\circ}$ denote the orientations that the dipolar axis is perpendicular and parallel to the surface, respectively. In this study, we attempt to obtain the distribution function of the angle for the surface water molecules. More specifically, we divide the θ angle (0° - 180°) into 32 regions and take the canonical ensemble average of the number of surface molecules falling into each region. The "surface molecules" here refers to the molecules located at top 3 $\mathring{A}$ from the surface.

The canonical ensemble average can be obtained by the Metropolis Monte Carlo method as described in the Introduction. In the model system the periodic boundary conditions are applied in x and y axes but not in z axis. Each cubic unit cell contains 256 water molecules and the length of the unit cell is chosen so that the density of water is equal to 1 g/cm^3. For the interaction potential, we consider both the ST2 and CI functions (see Introduction). In each case, the system is started from a slab-shaped liquid with hard wall constraint (i.e., the state (c) in Chapter IV). In the subsequent Monte Carlo steps, the hard walls are released. For each run, about 2×10^5 steps are called for. The results are shown in Figures 12 and 13. We note that for the

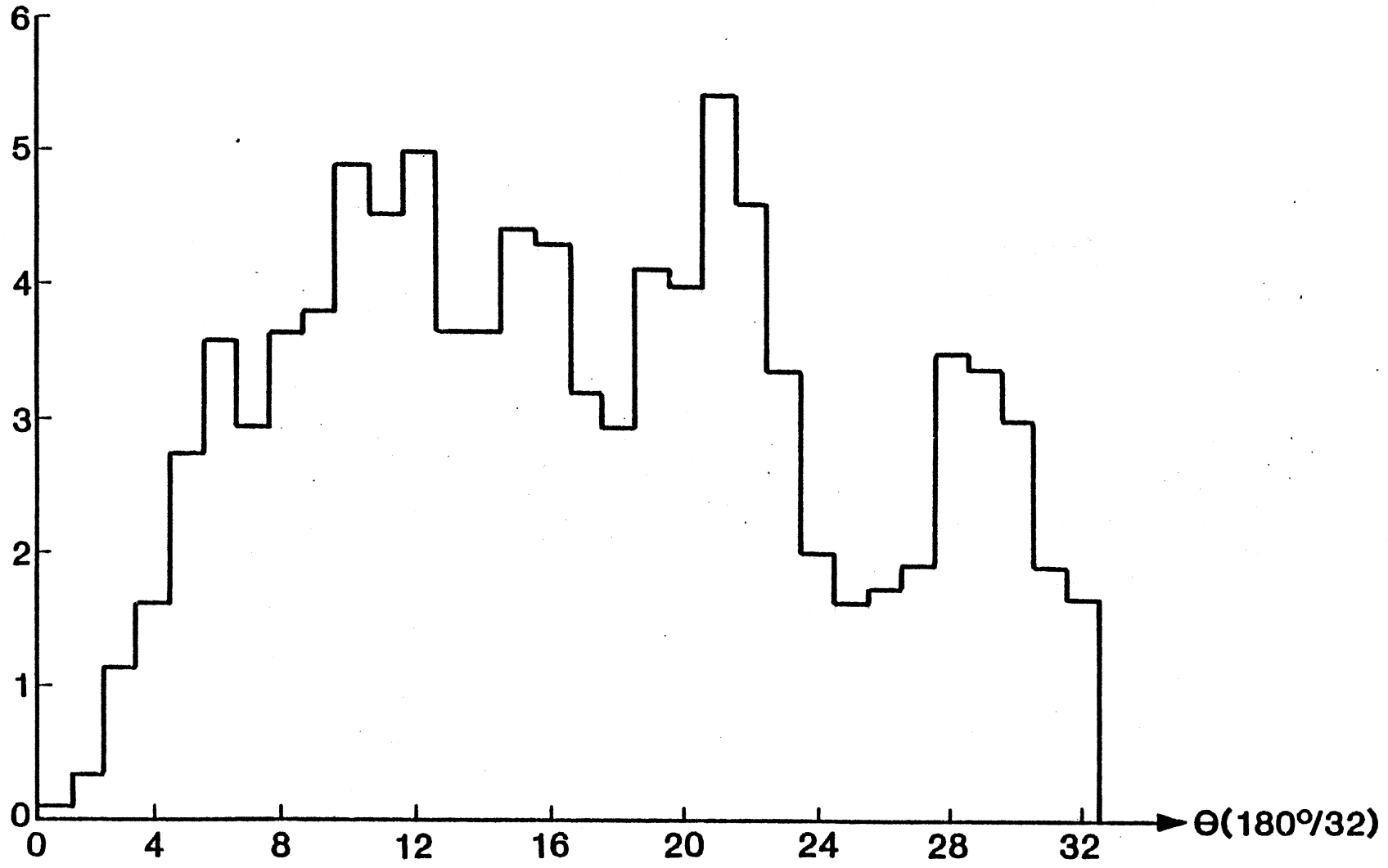

Figure 12. Orientational Distribution of the Surface Water Using ST2 Potential. The θ Angle is Divided into 32 Regions and the Vertical Axis Represents the Percentage of the Monte Carlo Steps Falling Into Each Region

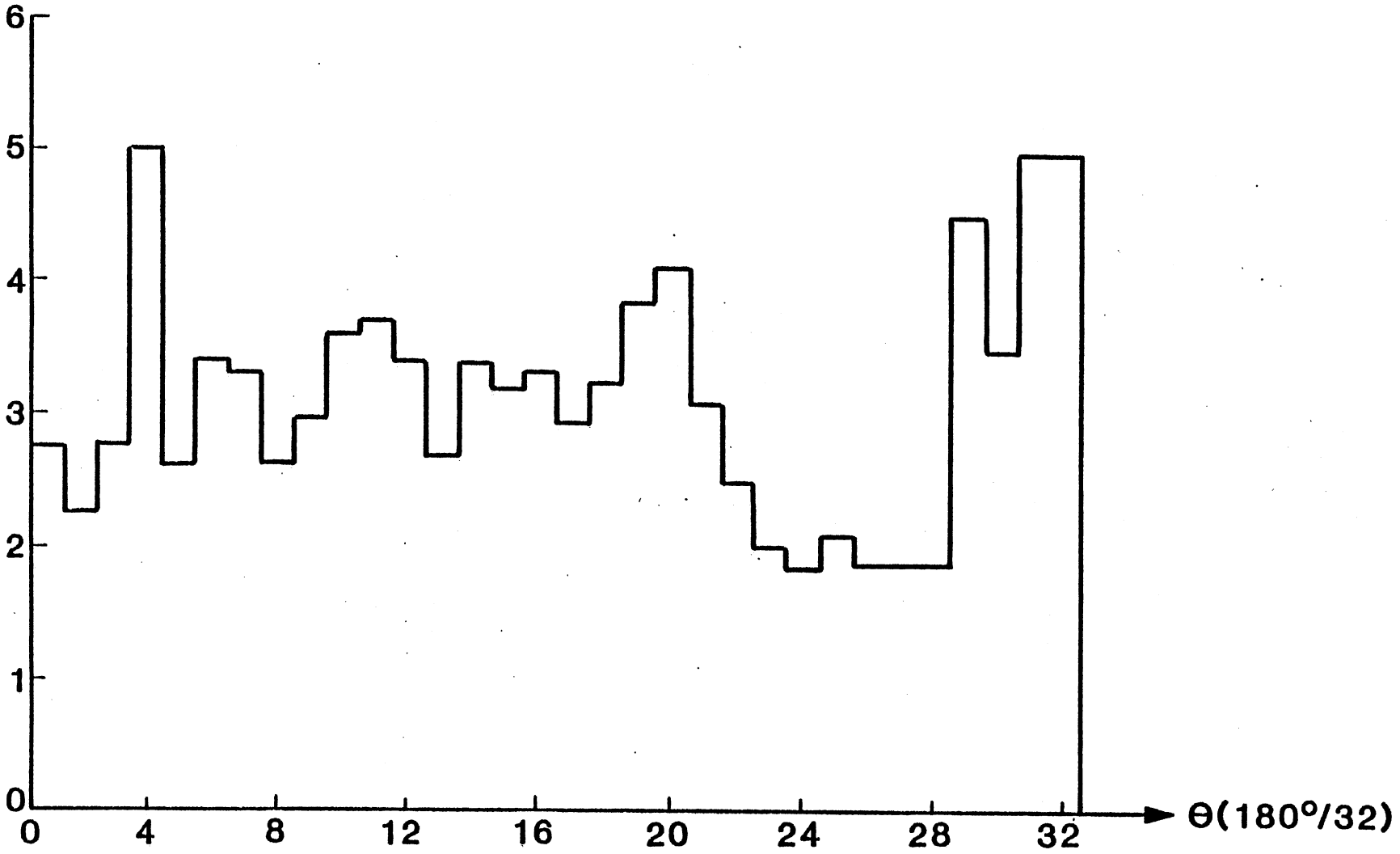

Figure 13. Orientational Distribution of the Surface Water Using CI Potential. The θ Angle is Divided into 32 Regions and the Vertical Axis Represents the Percentage of the Monte Carlo Steps Falling Into Each Region

CI potential the surface molecules are almost isotropic while for the ST2 potential the surface molecules tend to orient parallel to the surface. This is an interesting point for future experiments to test.

The surface structure of water should affect the structure of solutes. In our preliminary studies, we put a spherical dipole (radius = 3.5Å) at water surface and found that the dipolar solute also tends to orient parallel to the surface when the ST2 potential is used. The detailed orientational distribution still needs further elaboration.

VITA

Chyuan-Yih Lee

Candidate for the Degree of

Doctor of Philosophy

Thesis: A MONTE CARLO METHOD FOR THE CALCULATION OF THE SURFACE TENSION OF AIR-WATER AND LIPID-WATER INTERFACES

Major Field: Physics

Biographical:

Personal Data: Born in Tainan, Taiwan, June 13, 1948, the son of Mr. and Mrs. P. H. Lee.

Education: Graduated from Tainan First High School, Tainan, Taiwan, in June, 1966; received Bachelor of Science degree in Control Engineering from National Chiao-Tung University in June, 1970; received Master of Science degree in Physics from Tamkang College of Arts and Sciences in June, 1974; completed requirements for the Doctor of Philosophy degree at Oklahoma State University in December, 1980.

Professional Experience: Instructor, Department of Physics, Tamkang College of Arts and Sciences, 1974-1975; Graduate Teaching Assistant, Oklahoma State University, Department of Physics, 1977-1978; Graduate Research Assistant, Oklahoma State University, Department of Physics, 1978-1980.